UNIVERSITÄTSKLINIKUM HAMBURG-EPPENDORF

I. Medizinische Klinik und Poliklinik

Prof. Dr. med. Ansgar W. Lohse

Isolation of bile-derived extracellular vesicles using size exclusion chromatography in patients with biliary diseases.

Dissertation

zur Erlangung des Grades eines Doktors der Humanmedizin

an der Medizinischen Fakultät der Universität Hamburg.

vorgelegt von:

Sophia Kirstein

Hamburg 2024

Angenommen von der
Medizinischen Fakultät der Universität Hamburg am: 22.11.2024

Veröffentlicht mit Genehmigung der
Medizinischen Fakultät der Universität Hamburg.

Prüfungsausschuss, die Vorsitzende: Prof. Dr. Catherine Meyer-Schwesinger

Prüfungsausschuss, 2. Gutachter: Prof. Dr. Christoph Schramm

Inhaltsverzeichnis

1. Introduction

Biliary stenoses have a wide range of underlying causes, from iatrogenic, infectious, dietary, genetic, and congenital, to chronic inflammatory diseases such as primary sclerosing cholangitis (PSC), and malignant conditions like cholangiocarcinoma (CCA). Although these diagnoses indicate different implications in terms of treatment and prognosis, the clinical presentation is often similar, making the diagnostic differentiation so challenging.

The following gives a brief overview of clinical methods in use today to differentiate biliary stenoses, as well as the obstructing conditions relevant to the problem at hand: distinguishing between inflammatory and malignant biliary stenoses- in particular PSC and CCA because of their high comorbidity and poor prognosis of patients with PSC-associated CCA (PSC-CCA) (Grimsrud & Folseraas, 2019; Novikov, Kowalski, & Loren, 2019).

1.1. Clinical presentation of biliary stenoses

The most common clinical signs of biliary stenosis are symptoms of cholestasis. Patients often complain about jaundice, pruritus, and abdominal pain in the right upper quadrant, accompanied by elevated bilirubin, alkaline phosphatase and gamma-glutamyl transferase levels in blood tests. Also, acholia and bilirubinuria may appear (Bowlus, Olson, & Gershwin, 2016).

Since obstruction can be caused by any type of biliary stenosis, these symptoms rarely give any hint on the underlying cause or etiology. Also, the typical B-symptomatic triad, weight loss, fever, and night sweat can occur in both benign (e.g., in patients with chronic inflammatory diseases) and malignant stenoses, making a differentiation alone on clinical appearance impossible (Bowlus et al., 2016).

Medical history may give some clues about the significance of biliary stenoses. For example, history of cholecystectomy may be suggesting a post-surgical stenosis, while signs of chronic liver damage may be caused by a chronic inflammatory disease, and fatigue with malaise could suggest an underlying malignancy. However, some patients remain without any symptoms at all, eventually only displaying elevated cholestasis parameters in a routine blood test.

1.2. Clinical diagnostic

In general, the evaluation of undetermined biliary stenoses is an interdisciplinary effort, including a variety of diagnostic examinations, preferably following a clinical algorithm (Bowlus et al., 2023; Singh, Gelrud, & Agarwal, 2015; Xie et al., 2018). Usually, abdominal ultrasound is performed initially. However, there is often a lack of sufficient sensitivity to clarify the underlying cause (Grimsrud & Folseraas, 2019). In this case, cross-sectional imaging using computed tomography (CT) or magnetic resonance imaging (MRI) is necessary. But in comparison to MRI, CT displays a lower sensitivity. Especially when magnetic resonance cholangiopancreatography (MRCP) is used, which yields the highest sensitivity of up to 98% for the detection of biliary stenosis, and 75% for CCA in PSC patients (Charatcharoenwitthaya, Enders, Halling, & Lindor, 2008; Voigtlander & Lankisch, 2015). MRCP focuses on the right upper abdominal quadrant, depicting the liver, pancreas, gallbladder, and biliary tree. Heavily T2-weighted MRI sequences help visualize the hyperintense bile fluid, which would be pronounced by cholestasis and thereby enable high-resolution images. Furthermore, MRCP can rule out choledocholithiasis as a differential diagnosis by detecting intraductal stones at sizes as small as 2 mm (Altman & Zangan, 2016).

Endoscopic retrograde cholangiopancreatography (ERCP) is another standard diagnostic for the assessment and treatment of biliary stenoses. This endoscopic procedure for imaging and examining the bile and pancreatic ducts by local application of contrast medium can additionally be complemented by brush cytology and forceps biopsy. The reported sensitivity and specificity for malignancy of 70-90% and 50-90%, respectively, can be significantly improved by combining ERC with brush cytology, further supplemented by FISH analysis (Charatcharoenwitthaya et al., 2008; Trikudanathan, Navaneethan, Njei, Vargo, & Parsi, 2014; Xie et al., 2018).

In complex cases where no internal access is achievable, ERC can be replaced or combined with a percutaneous transhepatic cholangiography (PTC) or percutaneous transhepatic cholangiodrainage (PTCD) in a so-called “rendezvous procedure” for better access to the biliary tree. PTC, too, is an invasive imaging method for the biliary tree via contrast agent and an effective way of draining bile in case of severe cholestasis. It is important to note that cholestasis increases the risk for cholangitis, which, in severe cases, can progress to septic cholangitis with a high mortality risk.

For endoscopic ultrasound (EUS), a duodenoscope with an ultrasound transducer is brought close to the biliary tract and the pancreas, allowing the evaluation of the extrahepatic bile ducts and the pancreatic duct. EUS is commonly used for diagnosing choledocholithiasis, (chronic) pancreatitis, as well as gastric and hepatobiliary malignancies. Reported sensitivity and specificity for differentiation between malignant and benign stenoses is 97% and 88%, respectively, and EUS thus a very valuable tool for evaluating undetermined biliary stenoses. Another benefit of EUS is the possibility of obtaining tissue samples via fine needle aspiration (FNA) (Charatcharoenwitthaya et al., 2008; Rösch et al., 2004).

Cholangioscopy is another invasive method that, in addition to the possibilities of ERCP, allows a visual assessment of the bile ducts as well as the targeted acquisition of intraductal biopsies (Pereira et al., 2018).

Importantly, it has been shown that sensitivities and specificities of diagnostic methods for CCA detection decrease in presence of chronic inflammatory diseases, such as PSC (see Tab. 1).

Table. 1: Overview of sensitivity and specificity for different in-use diagnostic methods for diagnosis of CCA in PSC patients as reported in the literature.

	Sensitivity	**Specificity**	**References**
Sonography	57%	94%	(Charatcharoenwitthaya et al., 2008)
MRI/MRCP	89%	75%	(Charatcharoenwitthaya et al., 2008)
CT	75%	80%	(Charatcharoenwitthaya et al., 2008)
ERCP	91%	66%	(Charatcharoenwitthaya et al., 2008)
Brush cytology	43%	97%	(Taghavi, Eshraghian, Niknam, Sivandzadeh, & Bagheri Lankarani, 2018)
Forceps biopsy	30-84%	100%	(Voigtlander & Lankisch, 2015)
Cholangioscopy	33-65%	97-100%	(Song et al., 2020)

CA 19-9 (Cut-off value= 20 U/mL)	78%	67%	(Taghavi et al., 2018)

MRCP= magnetic resonance cholangiopancreatography, ERCP= endoscopic retrograde cholangiopancreatography, CA 19-9= carbohydrate antigen 19-9

All in all, there is a variety of diagnostic methods available for the evaluation of biliary stenoses. Yet, especially the differentiation between PSC and CCA remains difficult because large-duct PSC can manifest in single dominant stenoses, resembling the features of cholangiocarcinoma. This is of high importance since notably 46% of all patients develop dominant stenoses and 30% develop cholangiocarcinoma, making PSC a major risk factor for cholangiocarcinoma (Altman & Zangan, 2016; Novikov et al., 2019). Furthermore, PSC-CCA has a poor prognosis with a 5-year survival rate of under 20%. (Grimsrud & Folseraas, 2019).

1.2.1. Primary sclerosing cholangitis

PSC is a chronic progressive autoinflammatory disorder of the biliary tree of unclear etiology. It is characterized by chronic inflammation of the intra- or extrahepatic bile ducts or both, leading to cholestasis, fibrosis, and finally progression to cirrhosis and end-stage liver disease. There is no known treatment to alter the progression of the disease. Further, the risk of CCA is significantly increased in patients with PSC, leaving it the most feared complication of PSC.

Interestingly, PSC is more prevalent in northern Europe and less in Asia or southern Europe (Bowlus, Lim, & Lindor, 2019). According to a population-based study performed in Sweden, the incidence of PSC is estimated at 1.22 per 100,000 inhabitants with a point prevalence of 16.2 per 100,000 adult persons (Lindkvist, Benito de Valle, Gullberg, & Bjornsson, 2010). Additionally, 60-80% of all PSC patients are also diagnosed with chronic inflammatory bowel disease (inflammatory bowel disease), mostly resembling ulcerative colitis, displaying a further risk for colorectal carcinoma (Altman & Zangan, 2016; Shah et al., 2018).

The disease can be classified as either large- or small-duct PSC. However, with a share of 25-33% of all PSC patients, small-duct PSC is rather rare (Guerra et al., 2019). Furthermore, small-duct PSC is associated with a lower risk of hepatobiliary malignancy (Weismüller et al., 2017). Importantly, in small-duct PSC, imaging techniques are unable to visualize the inflammatory alterations and only a liver biopsy

can confirm the diagnosis (Liwinski & Schramm, 2018). In contrast, liver core biopsies are not commonly performed in patients with large-duct PSC. This is due to the rather unspecific histological signs and because the pathognomonic “onion-skin scar” of intrahepatic bile ducts cannot be found in all patients, probably due to the segmental infestation of PSC. Exceptions would be suspected overlaps of PSC with autoimmune hepatitis (AIH), which can be confirmed via biopsy. (Liwinski & Schramm, 2018).

Diagnosis of large-duct PSC relies foremost on cholangiographic features by MRCP and ERC, consisting of multiple short-segment stenoses with consecutive dilatations of the bile duct, which lead to a typical “beaded” appearance of the biliary tract. Since ERCP is associated with severe complications such as post-ERCP cholangitis, pancreatitis, perforation, and bleeding, MRCP is- despite its rather low sensitivity in early PSC stages- recommended as the primary imaging modality. ERCP is reserved for stenoses needing biosampling or a therapeutic approach (Aabakken et al., 2017; M. H. Chapman et al., 2019).

Further diagnostic evaluation of PSC patients includes both abdominal and endoscopic ultrasound for assessment of cholestasis, gallbladder-polyps, and liver fibrosis. EUS is especially suitable for imaging of the distal common bile duct and for non-invasive determination of the fibrosis stage, transient elastography is most frequently used (Liwinski & Schramm, 2018). Serum antibody diagnostics in patients with PSC consist of perinuclear antineutrophil cytoplasmic antibodies (p-ANCA), which can be found in about 93% of PSC patients without a sufficient specificity. In AIH or IBD, p-ANCA is also frequently positive. Other typical but unspecific signs of PSC are hypergammaglobulinemia, antinuclear antibodies (ANA) or smooth muscle antibodies (SMA) (Liwinski & Schramm, 2018).

Furthermore, due to the higher risk for CCA, regular assessment of biliary stenoses in patients with PSC is recommended. Here again MRCP is considered as primary screening method (Bowlus et al., 2023; Ehlken & Schramm, 2015). However, the ESGE recommends ERC with ductal sampling in form of brush cytology and biliary biopsies for diagnosis of suspected CCA in PSC patients. Also, if therapeutic ERC is performed in patients with dominant stenoses, ductal sampling should be performed (Aabakken et al., 2017).

This is also important since 30-50% of all patients develop CCA within the first year after PSC diagnosis (Song et al., 2020). Overall incidence of PSC-CCA ranges from 0.5 to 1.5 per 100.000 patients with PSC, indicating a significantly higher risk compared to the general population. Accordingly, the lifetime incidence for CCA in PSC patients is about 2-19.9% (Bergquist et al., 2023; Catanzaro, Gringeri, Burra, & Gambato, 2023).

PSC-CCA is mainly observed in extrahepatic bile ducts ((Catanzaro et al., 2023) and follows on bile duct dysplasia. Studies found 37% of liver explants from PSC patients after therapeutical transplantation displayed dysplasia. 83% of explants had BiIIN 2 or 3 (Lewis, Talwalkar, Rosen, Smyrk, & Abraham, 2010).

There is no cure for PSC, except for liver transplantation in patients with PSC-associated cirrhosis and end-stage liver disease. A recent study found 12.6% of a cohort of 227 PSC patients in need for a liver transplantation within 79 months of observation (Guerra et al., 2019). In transplant centers, the median time to either death or liver transplantation was estimated to be 9 to 18 years (Bowlus et al., 2019).

Stenoses can also be dilated therapeutically by balloon-dilatation or bridged with a stent during an ERC intervention. In cases of difficult access, PTC or a combination of ERC and PTC/PTCD can be considered. Drug treatment is limited to ursodeoxycholic acid, which is also used for primary biliary cholangitis and is administered for mitigating sequels caused by cholestasis. Evidence on other positive effects like increased survival time or slowing down progression remains divisive. The assignment of immunosuppressive drugs such as corticosteroids or azathioprine have not proven useful (R. Chapman et al., 2010).

Therapy of PSC-CCA follows the same guidelines as sporadic CCA with the exception that liver resection is regarded as unsuited for PSC patients with end-stage liver disease or cirrhosis (Saffioti et al., 2019).

1.2.2. Cholangiocarcinoma

With an annual incidence of 2.1 patients per 100.000 in western countries, CCA is the second most frequent primary hepatobiliary cancer and is causing 20% of the hepatobiliary malignancy related deaths (Forner et al., 2019; Moazzami et al., 2020).

CCAs are a heterogeneous group of intra- and extrahepatic, aggressive bile duct tumors. Considered risk factors include bile duct cysts, Caroli´s disease and inflammatory diseases such as PSC and other forms of cholangitis, as well as chronic hepatitis B and C infection. Also, lifestyle factors like obesity, diabetes, and excessive alcohol intake seem to play a role in carcinogenesis, however not as strong as the before mentioned factors (Khan, Tavolari, & Brandi, 2019). Importantly, there are differences in risk factors between intrahepatic (iCCA) and extrahepatic cholangiocarcinoma (eCCA). Hepatitis B and C infections for example showed a strong association with eCCA but less for iCCA. The same holds true for alcohol and for cholangiolithiasis (Khan et al., 2019).

Anatomically CCAs can be differentiated in distal- (dCCA), perihilary- (pCCA) and intrahepatic (iCCA) cholangiocarcinoma (Fig.1). However, since there is no specific ICD-10 code for pCCA, many studies only make a differentiation in intrahepatic and extrahepatic cholangiocarcinoma (Khan et al., 2019).

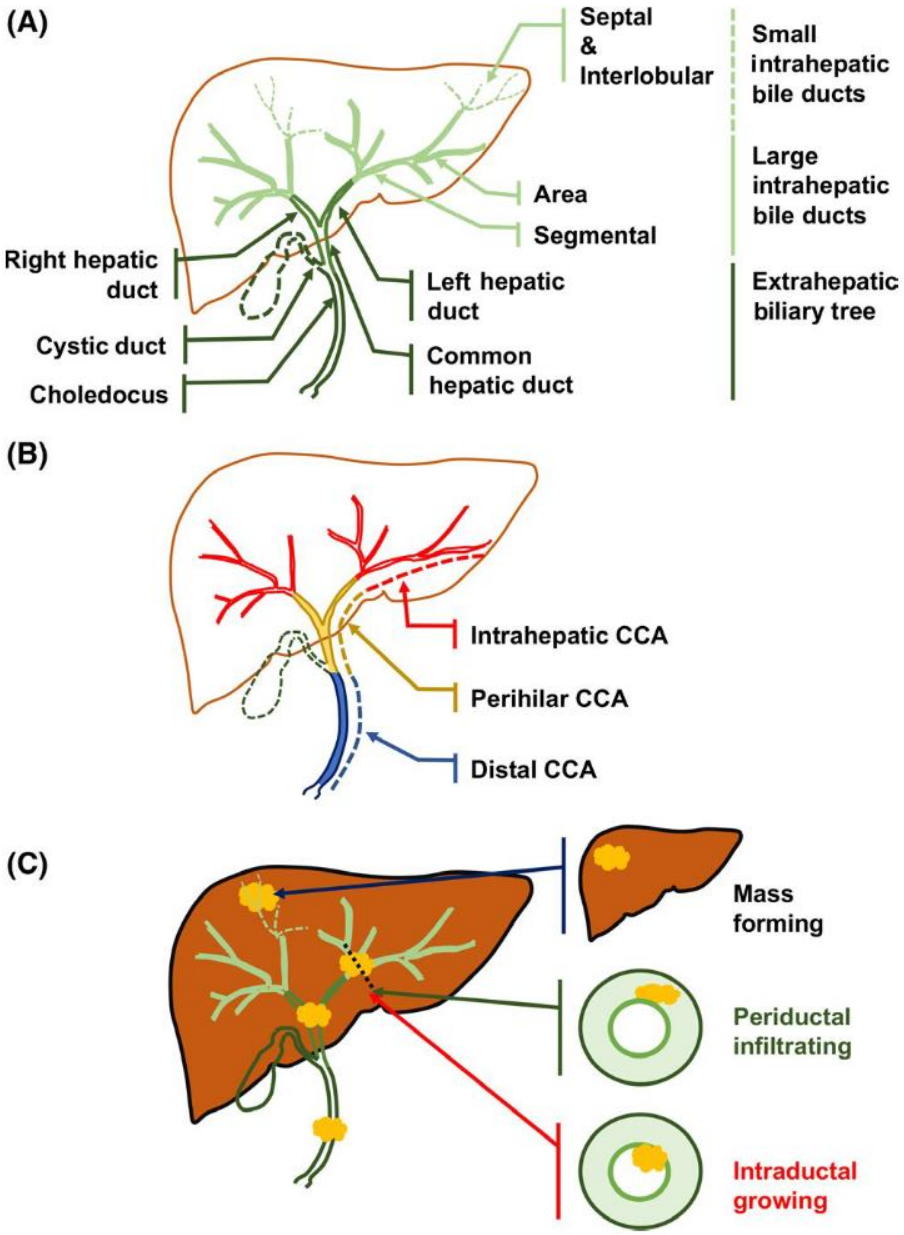

Figure 1: Overview over location, classification, and growing types of hepatic malignancies by Kendall et al. **(A)** Anatomical classification of the biliary tree in terms of small and large intrahepatic as well as extrahepatic bile ducts. **(B)** Scheme of cholangiocarcinoma (CCA) classification according to tumor location. Intrahepatic, perihilar, and distal cholangiocarcinoma are distinguished. Perihilar cholangiocarcinoma is the most common type of cholangiocarcinoma. **(C)** Different growing types of hepatic masses. Unlike intraductal growing tumors, periductal infiltrating and mass forming tumors do not cause biliary obstruction and therefore less symptoms. Especially mass forming tumors must be carefully investigated for both hepatocellular carcinoma and cholangiocarcinoma (Kendall et al., 2019).

pCCA, clinically also referred to as “Klatskin tumor”, is the most common type, accounting for about 50-60% of all CCAs. It is localized between the cystic duct and the second-degree branches. The second common location for CCA, with around 20-30%, is distal the cystic duct (dCCA) (Khan et al., 2019).

iCCAs represent about 10% of all CCAs and are therefore relatively rare (Kendall et al., 2019). These tumors are typically located in the smaller intrahepatic bile ducts after the bifurcation of the common bile duct. Importantly, since iCCA also invades the liver parenchyma, it can appear as a liver mass, unlike dCCA and iCCA, which only grow peri- or intraductal (Nakanuma et al., 2010). This increases the difficulty of distinguishing iCCA from hepatocellular carcinoma, complicated additionally by the similar risk factors and overlapping carcinogenic pathways (Kendall et al., 2019).

The diagnosis of CCA is based on imaging and histology for diagnostic confirmation. One of the high-resolution cross-imaging techniques is CT. Although it displays a higher sensitivity than abdominal ultrasound, the achieved 40-77% are still not sufficient for a faultless identification of malignant biliary stenoses. However, in case of malignancy, CT can simultaneously detect metastatic lesions, useful for cancer staging. Typical signs in CT for CCA are an increased thickness of the biliary duct wall over 1.5 mm, a hypo-attenuating biliary lesion during the arterial phase and biliary enhancement during the delayed phase, and long segment stenoses (Bowlus et al., 2016).

The only curative therapy for CCA is radical surgical resection. Unfortunately, most patients already show signs of tumor dissemination or distant metastasis by the time of diagnosis and are therefore unsuitable for surgical resection (Blechacz, 2017). In this case, chemotherapy with gemcitabine and cisplatin have shown to increase survival and therefore can be proposed in a palliative setting for all CCA types (Moazzami et al., 2020; Valle et al., 2009; Vogel et al., 2023). Furthermore, checkpoint inhibitors have also shown a life-prolonging effect in some studies (Kang, El-Rayes, & Akce, 2022). Therefor the anti-PD-L1 inhibitor durvalumab is now recommended by the European Society for Medical Oncology in combination with the above-mentioned chemotherapy regiment for therapy naïve patients (Vogel et al., 2023). Others include pemigatinib in case of Fibroblast growth factor receptor fusions or rearrangements (Abou-Alfa et al., 2020), and PD-1 inhibitors like pembrolizumab

(Deng et al., 2022), especially in cases of microsatellite instability (Kai et al., 2021). Further therapeutic methods include locoregional treatments such as radiofrequency ablation, hepatic arterial infusion chemotherapy, transarterial chemoembolization (TACE), drug-eluting bead-TACE, radioembolization, stereotactic radiotherapy, photodynamic therapy, and proton beam therapy (Moazzami et al., 2020).

Lastly, orthotopic liver transplantation (OLT) is a potential treatment for patients with CCA, especially pCCA which has proved to have the highest recurrence-free-5-year survival compared to the other modalities. However, the total 5-year survival rate was reported to be only 28% with high recurrence rates and OLT is only recommended in combination with chemotherapy (Moazzami et al., 2020).

In conclusion, CCA, including PSC-CCA, is a very aggressive tumor type, often mimicking benign PSC stenoses and displaying limited therapeutic options. Since curative treatment is only available in early stages, early diagnosis is key for improving survival in these patients. Biomarkers such as extracellular vesicles may add valuable information to increase the time of clinical diagnostic.

1.3. Extracellular vesicles

EVs are small membrane-enclosed spheres, which are present in body fluids such as serum, bile and urine (Julich-Haertel et al., 2017; Park et al., 2020; Severino et al., 2017), but also saliva and sputum, sperm, cerebrospinal fluid, breast milk, and tears (L. Li et al., 2014). According to their size, EVs are classified into exosomes, microvesicles and apoptotic bodies. Exosomes are the smallest EVs with an average diameter of 50-100 nm (Crescitelli et al., 2013). Size of microvesicles vary from 100 nm to 1 µm whereas apoptotic bodies are even larger with a range from 1 µm to 5 µm. Cells, in comparison, have a size of about 8-12 µm. Figure 2 gives an overview of the size distribution of EVs and other potential co-eluates.

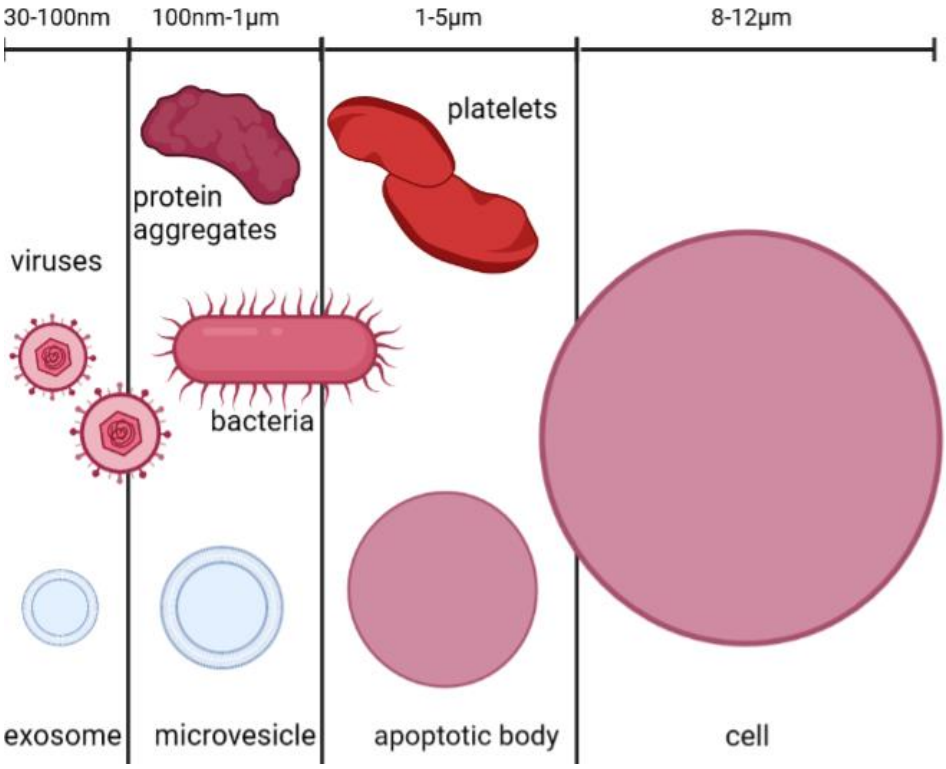

Figure 2: Size of different EVs (exosomes, microvesicles) in comparison with other possible components of body fluids after György et al. and created using Biorender.com. Dimensions are relevant in terms of sample purity after separating the samples using size exclusion chromatography. Most important in this regard seem to be protein aggregates, due to a similar size and potentially similar shape (Gyorgy et al., 2011).

Unlike microvesicles, which derive by direct budding from the plasma membrane of the cells, exosomes are secreted by the fusion of late endosomes or multivesicular bodies with the plasma membrane via SNARE proteins (Olaizola et al., 2018). Therefore, EVs contain specific subsets of proteins and lipids, as well as nucleic acids (DNA, RNA, and miRNA), cytokines, hormones and transcription factors (Colombo, Raposo, & Thery, 2014; Gradilone, 2017). However, the amount and content of EVs are also influenced by factors such as age, gender, BMI, disease, lifestyle, and medication (L. Li et al., 2014). EVs enable crosstalk between distant cells by paracrine ligand-receptor interaction or by horizontal transfer via endocytosis or fusion interaction with the plasma membrane (Choi, Kim, Kim, & Gho, 2015).

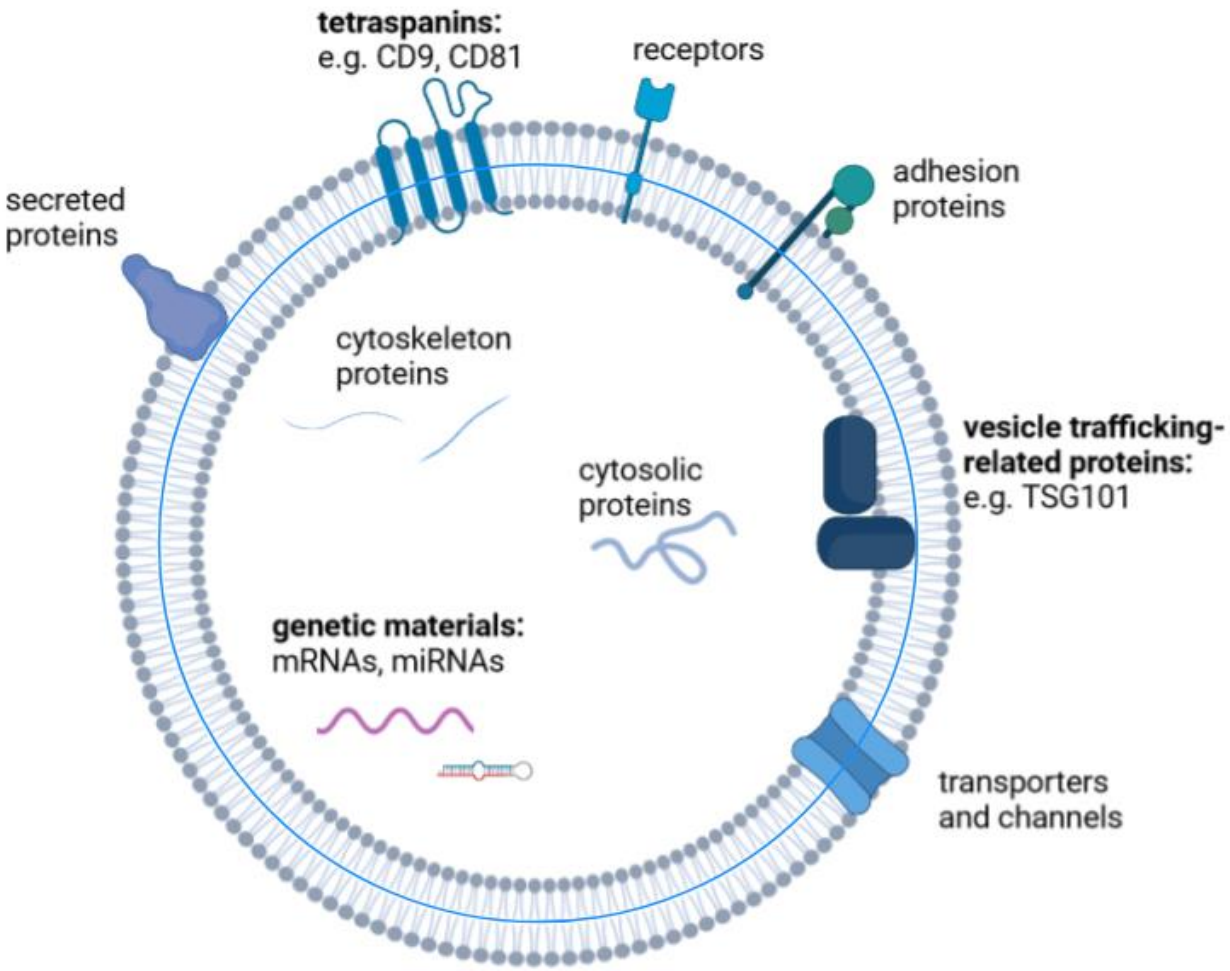

Figure: 3: Schematic image of EV structure after Choi et al. and created by using Biorender.com. Lipid membranes of EVs contain several transporter and channels next to receptors and adhesion proteins. Some of these proteins, such as tetraspanins and vesicle trafficking proteins like TSG101, can be used for EV detection via immunoblotting. Additionally, EVs typically contain various material from its original cell, such as cytoskeleton proteins, cytosolic proteins, and genetic materials. These can be used as biomarkers for several diseases (Choi et al., 2015).

Thereby, EVs play an important role in the regulation of cancer hallmarks, such as stimulating survival, tumor growth, and promoting inflammation (Haga et al., 2015). Previous studies showed that this crosstalk can promote tumorigenesis. For example, a mouse study showed modulation of intracellular growth mechanisms in cholangiocytes through interaction (L. Li et al., 2014). Furthermore, EVs induced migration and invasion through transfer of oncogenic proteins. And they transferred oncogenic proteins from mutated cholangiocytes to healthy cells (Gradilone, 2017).

At the moment, their potential lies in their use as biomarkers, especially since tumor cells have been found to secrete more EVs than healthy cells (Yoon & Chang, 2017). There are already studies on EVs as biomarkers for certain diseases, disease progression and sensitivity to chemotherapy (Stevic, Buescher, & Ricklefs, 2020). Lapitz et al. studied serum-derived EVs in PSC patients and found protein markers for CCA prediction and for prediction of overall survival (2023). The study of Olaizola et al. proposed EV-derived miRNA from serum as biomarkers for PSC (2018) and Severino et al. found EVs in bile more abundant in patients with malignant biliary stenoses compared to benign underlying diseases (2017). Further, Li et al. were the first to isolate miRNA in bile-derived EVs for differentiation between CCA and PSC (2014).

1.3.1 Isolation of extracellular vesicles

To date, ultracentrifugation (UC) is the most commonly used method of isolating EVs (Royo, Thery, Falcon-Perez, Nieuwland, & Witwer, 2020). The separation of the particles is carried out by different centrifugation steps with varying forces. For example, 300 g for the removal of cell debris and 100,000 g for sedimentation and concentration of EVs. Although UC has some advantages such as the possibility for high variance in sample size, the well-established protocols, and a lot of experience already gained, there are some disadvantages which made an alternative desirable (Ramirez et al., 2018).

Disadvantages of UC are the size and price of the centrifuge, the elaborate laboratory process, and, most importantly, the frequent contamination with proteins and RNA (Shao et al., 2018). The main contaminating particles are high density lipoproteins (HDL) and protein aggregates. Although HDLs only have a size of about 10 nm and are therefore significantly smaller than EVs, they have a similar density, which favors co-elution. Protein aggregates such as immune complexes, on the other hand, mimic EVs according to their size and are thus also present in the samples (Witwer et al., 2013). However, protein aggregates can be filtered out by ultrafiltration. Furthermore, studies claim that EV isolation is not suitable for clinical application with UC, and that the high speeds used during the process (>100,000 g) can destroy the EVs (Ramirez et al., 2018).

Here, size exclusion chromatography (SEC) offers a potential alternative to UC by separating proteins or other molecules based on their molecular size.

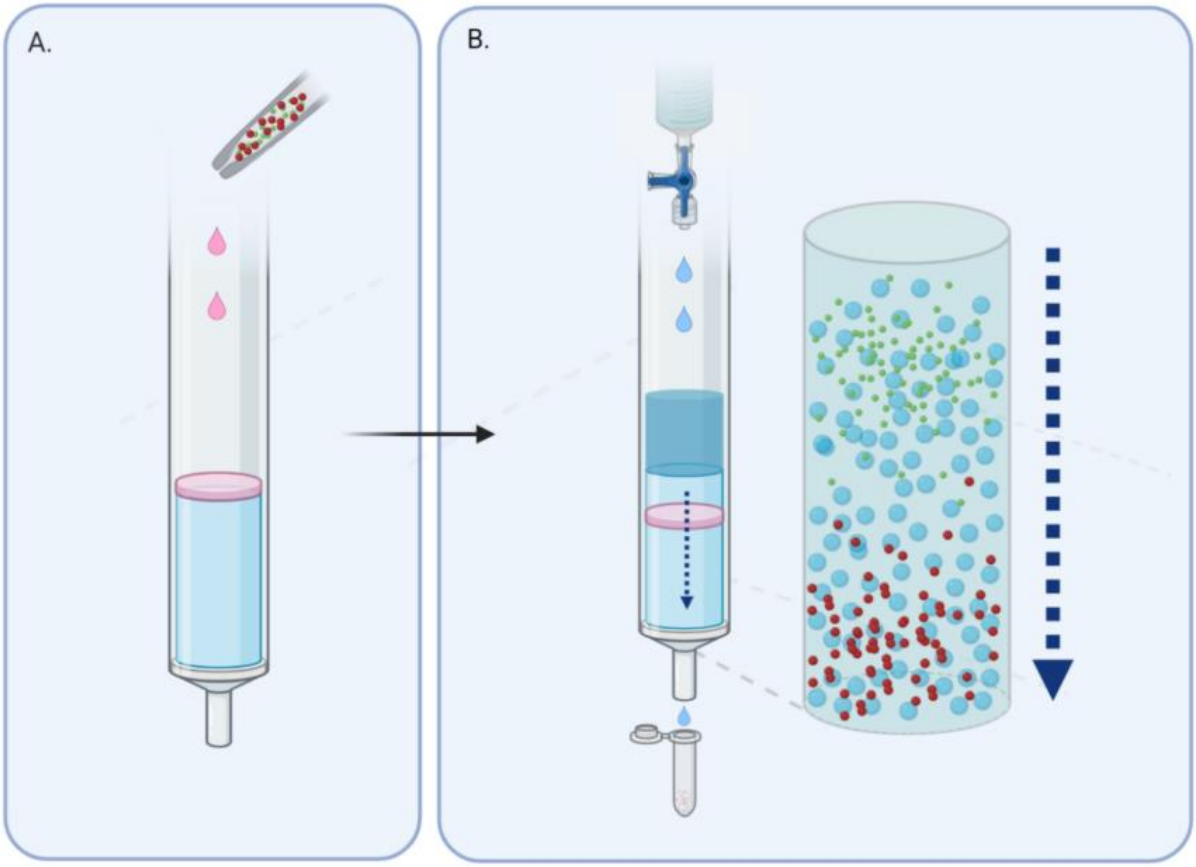

Figure 4: Principle of size exclusion chromatography by Liu et al. First, the sample is applied to the prepared column. Next, wash buffer is added to the column, facilitating sample flushing through the column. Inside the gel matrix of the column, particles are separated, making large particles (EVs, here in red) elute earlier than smaller particles (e.g., proteins, in green). Elution fractions are collected in tubes on the other side of the column (D. S. K. Liu et al., 2020). *EV= extracellular vesicles*

SEC columns consist of a solid matrix of permeable beads which get passed through by the liquid sample. The elution time depends on the individual speed of molecules by traversing the matrix. Large molecules cannot enter the pores and therefore remain in the liquid phase. This shortens their elution time. Conversely, small particles take longer because they initially get caught in the pores. This way SEC columns remove sample contaminants like viruses and DNA or protein aggregates (Cutler, 2004).

Parameters to consider when choosing from different SEC columns include pore diameter and matrix-type (e.g. high-resolution matrices with a narrow range of molecular-weight separation compared to wide ranges or other properties such as desalting) (Cutler, 2004). SEC columns used in this work (qEV, iZON, GE Healthcare) consisted of Sepharose for the optimal separation of EVs. The diameter of the pores was 75 nm, enabling molecules smaller than 75 nm to eluate late, while EVs with an average size of 100 nm eluate earlier.

SEC also has the benefit of effective separation of soluble proteins and EVs, and reduction of EV aggregation during isolation. Thus, in the purest fractions, a removal of 99% of the soluble plasma proteins and over 95% of HDL in blood samples was observed. In addition, isolation via SEC is claimed to preserve the biological activity and integrity of the EVs and is comparatively cheap (Ramirez et al., 2018).

However, a disadvantage is the high dilution of the samples after isolation, which requires ultrafiltration. Ultrafiltration and SEC are usually combined to concentrate the samples and thus to generate higher purity. Again, the biophysical properties and biological functions are reported to be unaffected (Ramirez et al., 2018).

SEC has been established for various body fluids such as serum, plasma, saliva, urine cerebrospinal fluid and cell culture media to isolate EVs (Izon, 2019) and EV-derived miRNAs (Coumans et al., 2017; L. Li et al., 2014; Navajas, Corrales, & Paradela, 2019; Park et al., 2020). Whether EVs can be effectively isolated by SEC from bile to analyze miRNA and proteomics remained to be tested.

1.4. MicroRNA

MiRNAs are short (around 20 to 22 nucleotides long) non-coding RNAs, which regulate protein translation by mRNA silencing (Letelier et al., 2016; Lu et al., 2005). Due to their ability to regulate cell differentiation, apoptosis, and proliferation, miRNAs play an important role in inflammation and carcinogenesis (Garzon, Marcucci, & Croce, 2010; Iorio & Croce, 2012; Lu et al., 2005). Thus, miRNAs have been found to function both as tumor suppressors and oncogenes.

The biogenesis of miRNA depends on different enzymes and processing steps (Fig. 5) and is related to different developmental cell states (Letelier et al., 2016). In

general, the transcription of miRNA to pri-miRNA (primary transcripts) occurs by RNA polymerase II or III. The genes for miRNA expression are localized in the intron and can be transcribed either individually or in tandem by polycistronic sequences. This allows simultaneous expression of multiple miRNAs. Only a few miRNAs have a specific promoter region and are regulated by transcription factors. The conversion of pre-miRNA to miRNA takes place after transport into the cytoplasm. From there, they can either be released by EVs or to the extracellular matrix and other cells, such as ribonucleoproteins and argonaut proteins (Letelier et al., 2016).

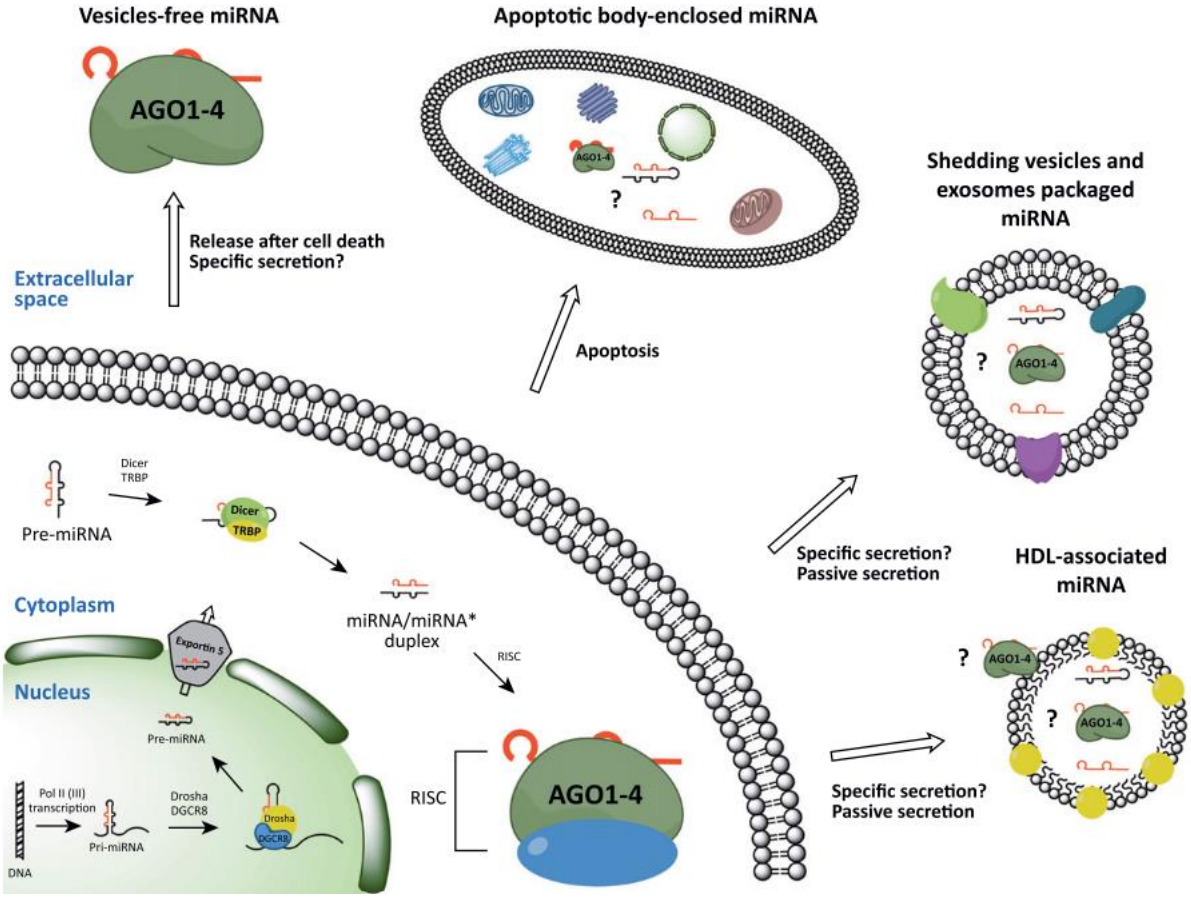

Figure 5: Overview over biogenesis of miRNAs in the cell and the modes of extracellular miRNA packaging by Turchinovich et al. Briefly, miRNAs are synthesized by RNA polymerase II or III, firstly to pri-miRNAs located in the nucleus. After maturing to pre-miRNAs, they are transported into the cytoplasm where miRNA duplexes are formed. Lastly, the guide miRNA strand binds to an argonaut protein (AGO) and is released into the extracellular space, either vesicle free or enclosed in apoptotic bodies, exosomes, or HDL. Question marks highlight open questions, such as if exosomes also contain pre-miRNA and protein-free miRNA, and where exactly

miRNAs are located in HDL. Either on the surface or incorporated inside (Turchinovich, Weiz, & Burwinkel, 2012). *HDL= high density lipoproteins, RISC= RNA-induced silencing complex*

Due to alterations in expression and their stability, miRNAs are predestined as biomarkers. For example, low expression of miRNA in cancer cells has shown to suggest a role as tumor suppressor, while overexpressed miRNAs are considered pro-tumorigenic, either by promoting apoptosis of tumor suppressors or by stimulating cell proliferation (Letelier et al., 2016).

Accordingly, different patterns of circulating miRNA, isolated from serum (Bernuzzi et al., 2016; Voigtlander et al., 2015) and bile (Shigehara et al., 2011; Voigtlander et al., 2015) have shown to be promising markers with diagnostic potential for CCA, PSC, and other biliary diseases.

Importantly, miRNAs are also present in EVs. The advantage of transport by EVs is the higher protection against RNase. It turned out that their half-life in circulation could be increased when enclosed in EVs (Letelier et al., 2016). Accordingly, the potential of some EV-derived miRNAs as biomarkers has already been recognized. The study of Li et al. investigated miRNAs from bile-derived EVs isolated via ultracentrifugation. They established a panel of 5 miRNA markers for diagnosis of CCA diagnosis with a sensitivity and specificity of 67% and 96%, respectively (L. Li et al., 2014)

In our study, we investigated selected miRNAs associated to tumorigenesis. MiR-1281 and miR-640 have been shown to have tumor suppressive potential. MiR-1281 for example, has been proposed to function as a tumor suppressor in different cancer types, such as bladder cancer (Pignot et al., 2013), osteosarcoma (Jiang et al., 2018), gastric carcinoma (G. Liu, Jiang, Qiao, & Wang, 2019) and colorectal carcinoma (Lv, Zhou, & Liu, 2021; Zhang et al., 2019), being downregulated in cells when measured with quantitative RT-PCR. Jiang et al. found a connection between miR-1281 and the tumor suppressor p53 with the latter being directly bound to the promoter of the miRNA, leading to its increase under stress of the endoplasmic reticulum (2018). Interestingly, miR-1281 was also found in serum exosomes of patients with colorectal carcinoma and its expression was also significantly downregulated in cancer patients (S. Yan et al., 2017).

MiR-640 seems to inhibit carcinogenesis for example in hepatocellular carcinoma by inhibiting the HIF-1a signaling pathway (Zhai et al., 2019) and in breast cancer via the Wnt7b/b-catenin signaling pathway (Tang et al., 2021). Furthermore, miR-640 was found downregulated in tissue of patients with serous ovarian carcinoma (X. Li, Lu, Chen, Lu, & Xie, 2013) and seems to play an inhibiting role in angiogenesis and therefore tumor progression (Harel, Sanchez-Gonzalez, Echavarria, Mayaki, & Hussain, 2020).

MiR-412 on the other hand, was found increased in serum of patients with squamous cell lung carcinoma (Gao et al., 2011) and in saliva-derived exosomes of patients with oral squamous cell carcinoma (Gai et al., 2018). One pathway, influenced by miR-412 influencing tumor immune response, was identified to be the toll-like receptor signaling pathway in patients with clear cell renal cell carcinoma (Wang et al., 2020).

Lastly, all the three miRNA markers were analyzed for their ability to distinguish PSC from PSC-CCA in a global miRNA profiling model. MiR-1281 displayed a specificity of 90% when analyzed in serum, while miR-412 and miR-640 isolated from bile yielded 89% and 92%, respectively (Voigtlander et al., 2015).

1.5. Aim of the study

This study aimed to investigate the feasibility of SEC for bile-derived EVs by characterizing EVs via nanoparticle tracking analysis (NTA), immunoblotting, and transmission electron microscopy (TEM). Further, we tested isolated EVs for established miRNAs associated with CCA that could serve as future biomarkers (Voigtlander et al., 2015). Additionally, eluted proteins were evaluated for their potential as biomarkers for CCA, e.g., after proteomic analysis.

2. Ethical Approval

The study was approved by the Ethics Committee of the Hamburg Medical Association (approval number 2021-10467-BO-ff).

3. Material

3.1. Machines and Devices

Biofuge B Microcentrifuge (4°C)	Heraeus sepatech, Germany
Blotting chamber 41-2340	Peqlab, Germany
Blotting rack	BioRad, USA
BVC vacuum pump	Vacuubrand, Germany
Centrifuge Rotana 460S	Hettich, Germany
CO_2-Incubator (37°C)	Sanyo, Japan
Dri-block DB-3D	Techne, USA
Elisa Microplate reader	Tecan, Switzerland
Fusion TX	Vilber lourmat, Germany
Gel bracket	BioRad, USA
Gel comb 10x0,5mm	BioRad, USA
Gel fixator	BioRad, USA
Glass plate 0.75mm	BioRad, USA
Glass plate 1.5mm	BioRad, USA
Glow discharge unit	Pelco, USA
Microcentrifuge 5427R	Eppendorf, Germany
myFuge 12 Mini Centrifuge	Benchmark Scientific, USA
NanoSight LM10	Malvern Panalytical, UK
Peqstar Thermocycler	Peqlab, Germany
PowerPac Basic Power Supply	BioRad, USA
Qubit fluorometer	ThermoFisher, USA
Running chamber 41-2340	Peqlab, Germany
Scale 822	Kern, Germany
Sonoplus sonification device	Bandelin, Germany
Tuberoller RS-TRO 5	Phoenix, Germany
Viia 7 Real Time PCR System	AppliedBiosystems, USA
Vortex shaker VF2	IKA, Germany

3.2. Chemicals

Aprotenin	Roth, Germany
Benzamidin	Sigma, Germany
Bromphenol blue	Sigma, Germany
DTT	Roth, Germany
EDTA	Böhringer Ingelheim, Germany
Emplura 2-Propanol	Merck, Germany
ETOH 100	Chemsolute, Poland
ETOH 70	Roth, Germany
Glycerin	Roth, Germany
Glycerol	Sigma, Germany
HCl	Sigma, Germany
HEPES	Sigma, Germany
Leupeptin	Roth, Germany
NaCl	Roth, Germany
NaF	Sigma, Germany
Natriumorthovanadat	Sigma, Germany
PBS	Sigma, Germany
PMSF	Sigma, Germany
Ponceau-S solution	AppliChem, Germany
Rotipherese Gel 40	Roth, Germany
SDS	Roth, Germany
ß-Mercaptoethanol	Roth, Germany
TEMED	BioRad, USA
Trisma Base	Sigma, Germany
Triton X	Merck, Germany
Tween	Sigma, Germany
Uranylacetat powder	EMS, Brasil

3.3. Kits

AllPrep DNA, RNA, miRNA Kit	Qiagen, Germany

BCA Assay Kit	ThermoFisher, USA
High-capacity cDNA Reverse Transcription Kit	Applied Biosystems, USA
Qubit micro-RNA assay kit	ThermoFisher, USA
RealTimePCR System StepOnePlus	Applied Biosystems, USA

3.4. Consumables

Amicon Ultra-15 Filter Unit	Merck-Milipore, Germany
Carbon-coated grids	Sigma, Germany
Falcons (15 mL)	Greiner Bio One, Austria
Falcons (50 mL)	Greiner Bio One, Austria
Filtorpur Bottle Top Filter 0.2 µm	Sarstedt, Germany
MicroAmp Fast 96-Well Reaction Plate (0.1 mL)	Applied Biosystems, Germany
Microcentrifuge tubes (2 mL)	Eppendorf, Germany
PCR Singe Cap 8er Soft-Strips 0.2 mL	Applied Biosystems, USA
Pipet-Boy	Integra, Germany
Protran Nitrocellulose membrane 0.45 µm	GE Healthcare, Germany
qEV2 column 70 nm	Izon, New Zealand
Receiver Bottle 500 mL	Sarstedt, Germany
Tweezer	GE Healthcare, Germany
Whatman Gel Blot Paper	GE Healthcare, Germany

3.5. Antibodies and Primer

Antibody CD9 mouse [106261] Antibody CD9 rabbit [13174] Antibody CD9, mouse [10626D]	ThermoFisher, USA Cell Signaling, USA Invitrogen, USA
Antibody TSG 101 rabbit [A303-507A]	ThermoFisher, USA
Cel-miR 39-3p [A25576]	ThermoFisher, USA

HRP-linked Antibody, anti-mouse [7076]	Cell Signaling, USA
HRP-linked Antibody, anti-rabbit [7074]	Cell Signaling, USA

Page Ruler Prestained Protein Ladder	ThermoFisher, USA
Taqman MicroRNA Assay miR-2181	ThermoFisher, USA
Taqman MicroRNA Assay miR-39	ThermoFisher, USA
Taqman MicroRNA Assay miR-412	ThermoFisher, USA
Taqman MicroRNA Assay miR-640	ThermoFisher, USA

3.6. Buffer and Gels

For BCA Analysis

Protein lysis buffer	1L
- HEPES	11.91 g
- NaCl	8.77 g
- H_2O	ad 900 mL
- Triton X	1%
- NaF	50 mM
- 0.5M EDTA pH 8.0	2 mM
- Glycerol	100 mL
Proteinase inhibitors:	to 50 mL buffer
- Benzamidin	10 nm
- Natriumorthovanadat	2 nm
- Leupeptin	1 µg/mL
- Aprotenin	3.5 µg/mL
- PMSF	1 mM

For Immunoblotting

Separation gel 12% stock (100mL)	
- H2O	24 mL
- Acrylamide 40%	30 mL
- 1.5M Tris pH 8.8	25 mL

- 10% SDS - Glycerol For 2 gels 1.5 mm	1 mL 20 mL
Collection gel stock - H2O - Acrylamide 40% - 1M Tris pH 6.8 - 10% SDS for 2 gels 1.5mm	100 mL 74 mL 12.5 mL 12.5 mL 1 mL
Running buffer 10x - SDS - Glycine - Tris base - H2O	 20 g 288 g 60.6 g ad 2 L
Blotting buffer 10x - Glycine - Tris base - H2O	 144 g 30.3 g ad 1 L
TBS 10x (pH 7.6) - Tris base - NaCl - dH2O - 13M HCl	 24.22 g 175.32 g 2 L 14.5 mL
Blocking solution - 10x TBS - Tween - Milk	 ad 1 L 0.05% 5%
Antibody solution - 10x TBS - Tween - BSA /milk	 ad 1 L 0.05% 5%
Washing buffer - 10x TBS	 ad 1 L

- Tween	0.05%
Sample buffer (Laemmli 5x) - Tris base - SDS - Bromphenol blue - Glycerol - DTT - H_2O	50 mL 1.5 g 5 g 250 g 25 mL 3.86 g ad 50 mL

3.7. Software

BCA ELIZA	i-control 1.10 f50
NTA	NTA software 3.0
qPCR	ViiA 7

4. Methods

4.1. Patient data

9 patients with biliary stenoses undergoing ERC were included to the study. The patients could be categorized into three groups of 3 patients each, defined by their underlying conditions (malignant, chronic inflammatory and benign-non-inflammatory). For these patients, clinical data including laboratory results (transaminases, total bilirubin, CRP, and CA 19-9) were documented.

Before, bile and serum samples from patients with different diseases were collected and used for method implementation. Patients who did not gave informed-consent and children (age < 18 years) were not considered for this study.

Bile samples were obtained from patients with biliary stenoses undergoing ERC or PTCD in the University Hospital Hamburg Eppendorf between 2019 and 2020. Aspiration of bile from the biliary system was performed before injection of contrast agent. Samples were collected, aliquoted, and stored at -80°C without any further additions prior to analysis.

Blood samples were also obtained from patients undergoing ERC shortly after the procedure. Whole blood was then separated by centrifugation at 1800 rpm for 10 minutes and serum samples were stored as well at -80°C.

A graphical workflow of this study is demonstrated below (Fig. 6)

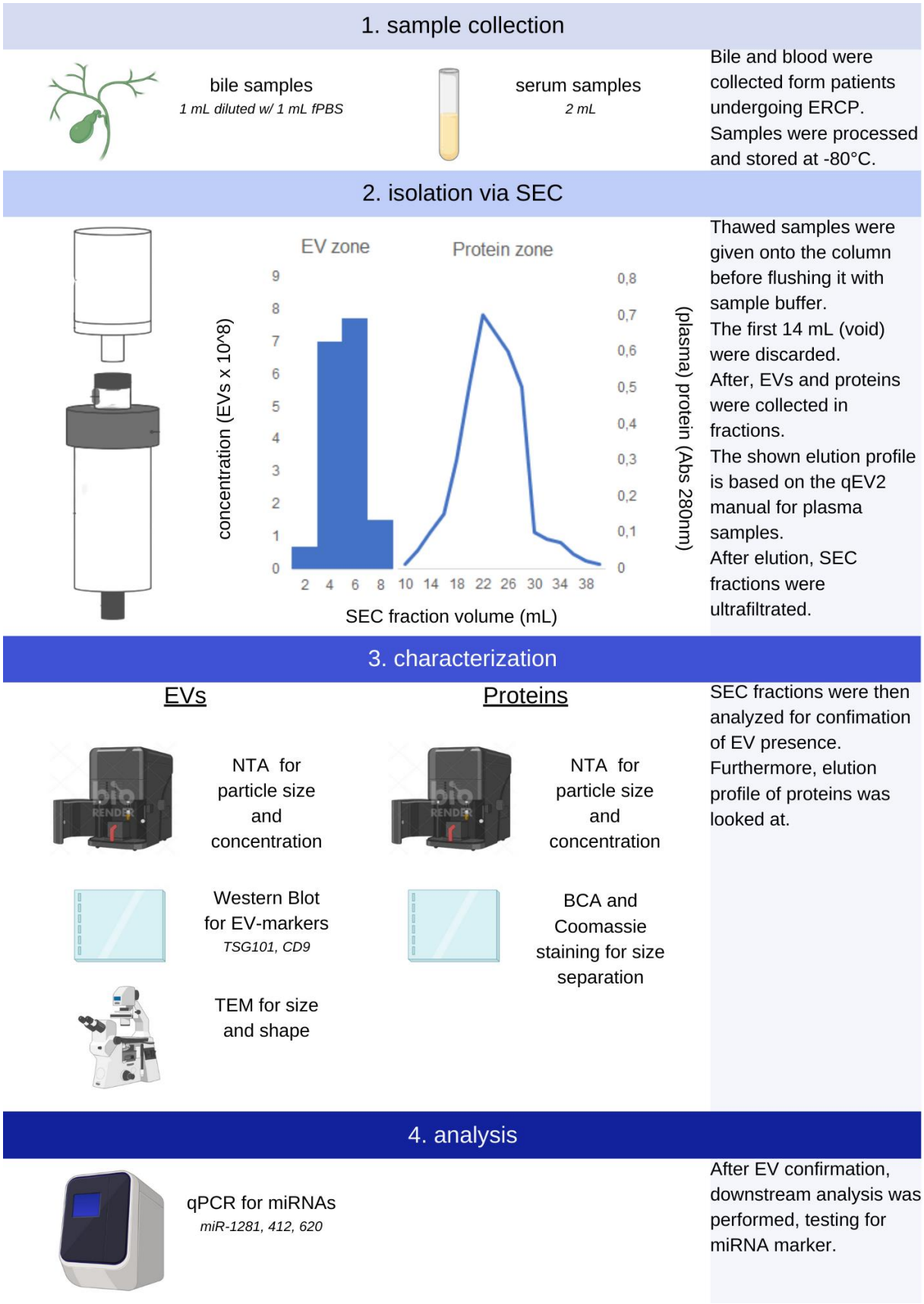

Figure 6: Graphical workflow created using Biorender.com.

(1) First, sample collection of bile, obtained by ERCP and serum, was performed, followed by preparatory steps before applying the sample to the SEC column. Preparatory steps included dilution of bile to reduce viscosity and centrifugation of both bile and serum to eliminate cell detritus and other large components. **(2)** Next, EV were isolated via SEC. EV fractions were defined as the first fractions, containing the first 8 mL after void elution. After, protein fractions were collected up to a peak after 26 mL after void elution. EV fractions were ultrafiltrated after the elution process in order to concentrate the sample. **(3)** Subsequently, both EV and protein fractions were characterized. EVs samples were validated for EVs, using NTA, Immunoblotting and TEM. Protein fractions were analyzed using NTA and BCA-assay. **(4)** After validation of EV abundance in the EV fractions, miRNA was isolated from the fractions using quantitative RT-PCR looking at specific biomarkers previously described in PSC-CCA patients. Both EV and protein fractions were processed for proteomic analysis. *ERCP= endoscopic retrograde cholangiopancreatography, SEC= size exclusion chromatography, EV= extracellular vesicle, NTA= Nanoparticle tracking analysis, TEM= Transmission electron microscopy, BCA= bicinchoninic acid, RT-PCR= Real Time Polymerase Chain Reaction, PSC-CCA= Primary-Sclerosing-Cholangitis-associated Cholangiocarcinoma, fPBS= filtered PBS*

4.2. Extracellular vesicles

4.2.1. EV isolation

Extracellular vesicles were isolated from 1-2 mL thawed bile and serum. Serum samples were used as control since SEC columns are officially feasible for serum samples. For cell depletion, bile was centrifuged for 10 minutes first at 1200 g, the supernatant was kept and centrifuged again for 10 minutes at 10000 g. For decreasing viscosity of bile, the sample was diluted 1:1 with filtered PBS.

For isolation via SEC qEV2 columns (Izon) with a pore size of 70 nm were used. Briefly, columns were brought to room temperature and flushed with freshly filtered PBS. Fraction collection started after applying the bile or serum sample. However, the first 14 mL were considered as void volume according to the manual and were discarded. The next 8 mL were considered as EV zone and were collected in 2 mL fractions (EV1, EV2, EV3 etc.). Particles which eluted later were considered

belonging to the protein zone and were collected in 5 mL fraction (P1, P2 etc.). EV and protein fractions were concentrated to about 400-500 µL using ultrafiltration filters 15 kDa (Amicon), centrifuging 3500 g for 30-60 minutes. An overview over sample and fraction sizes for EV isolation procedures including performed downstream analysis done in this study can be found in Supplementary Table 1.

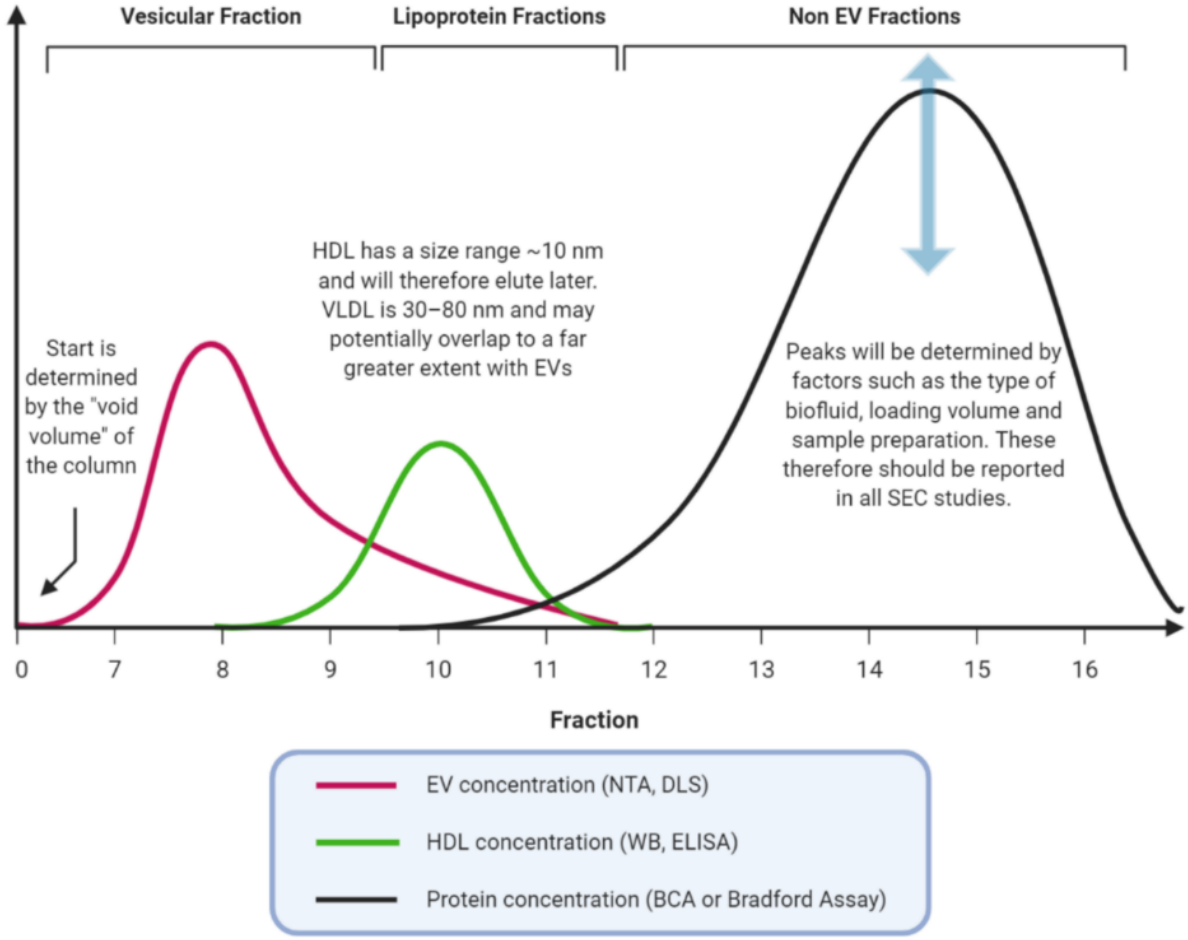

Figure 7: Typical elution profile with consecutive fractions by Liu et al. Fractions are given in mL after void elution, identifying the Vesicular Fraction or EV zone with the highest EV yield as the first 8 mL after void elution. After 8 mL, lipoproteins will start to elute, displaying the risk of contamination in EV downstream analysis. Lastly, proteins will elute from the SEC column, concentration and fractions depending on the used sample. The legend indicates the methods feasible for concentration measurements of different fraction types (D. S. K. Liu et al., 2020). *NTA= nanoparticle tracking analysis, DLS= dynamic light scattering, HDL= high-density lipoproteins, WB= western blot, ELISA= enzyme-linked immunosorbent assay, BCA= bicinchoninic acid.*

4.2.2. Immunoblotting

Immunoblotting is the gold standard for the detection of EVs in samples. It enables the detection of surface-typical proteins on EVs. However, immunoblotting cannot perform a quantitative analysis of EVs. Additionally, it is important to note that these proteins are not EV specific, but only typical for EVs. Furthermore, contamination of the samples cannot be assessed via immunoblotting (Witwer et al., 2013).

Immunoblotting was performed for detection of EV markers TSG101 and tetraspanin CD9.

For immunoblotting fractions EV1-4 were pooled to obtain a clearer signal. Protein concentration was measured via BCA assay as described above.

Next, sample buffer/Laemmli 5x was added to a sample aliquot, containing approximately 10-15 µg protein and heated 5 minutes at 95°C for denaturation, before placing on ice again.

Separation and collection gels were produced following the instructions above and poured between a 1.5 mm and 0.75 mm glass plate, fastened with a fixator in a gel bracket. Collection gel was poured on top without producing any bubbles and a gel comb with 10 wells 1.5 mm was inserted. Gels were rested for 30 minutes to allow polymerization.

Next, samples were loaded onto the gel next to 5 µL protein ladder. Until separation of protein ladder (15 min at 100 V), the gel ran for 1-1.5 h at 160 V. Afterwards the gel was transferred to a nitrocellulose membrane by blotting for 1 h at 300 mA. Correct blotting was confirmed by Ponceau staining. The membrane was then blocked (Tab. 2) for 1 h and incubated with the primary antibody overnight. Secondary antibody was applied the next day after several washing steps 1:2000 in 5% milk for 1 h at room temperature. FusionFX was used for imaging after incubation with 3 mL ECL solution for 5 min. For stripping, the membrane was incubated in Stripping Solution for 30 minutes.

Table 2: Primary antibodies used for immunoblotting and their blocking conditions, according to the manufacturer's manual.

Primary antibody	Blocking condition	manufacturer
Antibody CD9, mouse [106261] Antibody CD9, rabbit [13174] Antibody CD9, mouse [10626D]	1:1000 in 5% BSA 1:1000 in 5% BSA 1:500 in 5% milk	ThermoFisher, USA Cell Signaling, USA Invitrogen, USA
Antibody TSG 101, rabbit [A303-507A]	1:500 in 5% BSA	ThermoFisher, USA

4.2.3. Nanoparticle tracking analysis

NTA of EV samples was conducted to determine the size and concentration of EVs in the eluted fractions. NTA is a method of optical tracking of nanoparticles to measure their size and concentration. A beam of light illuminates the particles in the sample, which is reflected due to Brownian molecular motion of the particles. The camera can track these individual light reflections and use them to calculate the average speed and diffusivity. From this calculation, the estimation of the size and particle concentration is carried out (Shao et al., 2018). In addition, the device is coupled with a microscope, which makes direct visualization with a magnification of 20x possible. Generally, NTA can detect particles in sizes from 10-2000 nm.

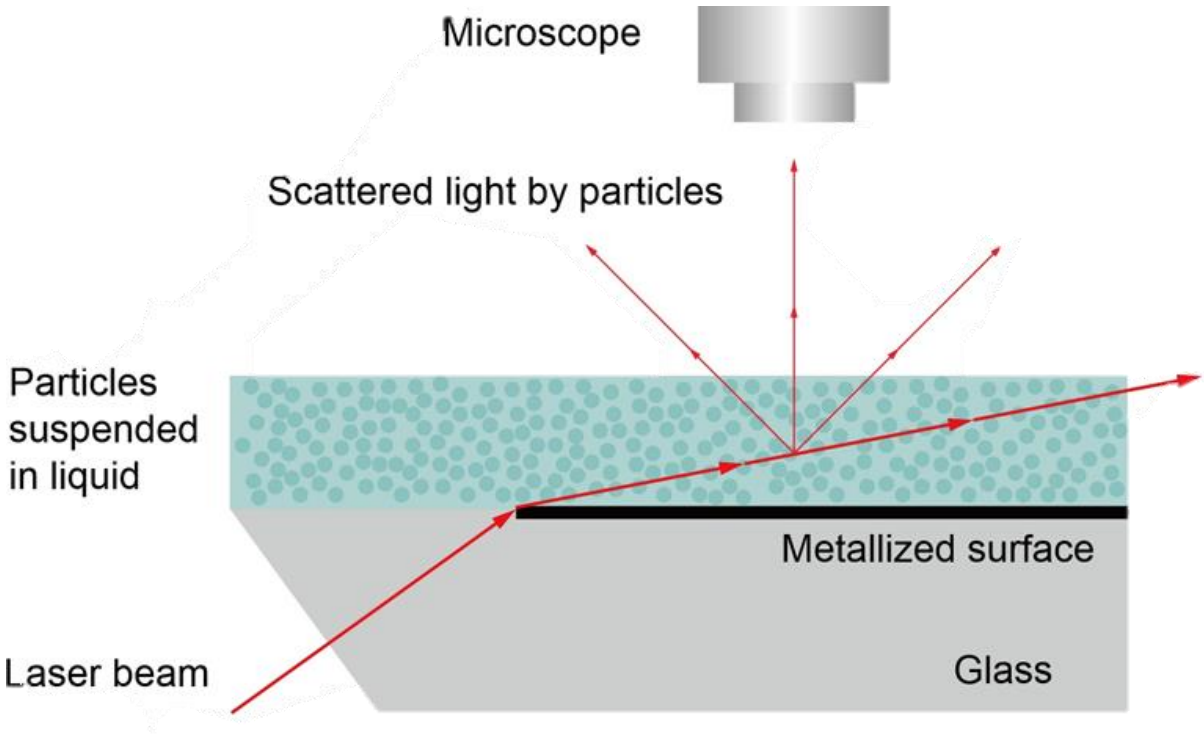

Figure 8: Schematics of Nanoparticle tracking analysis, derived from a graphic by Kim et al. The sample is injected into the chamber opposite to the magnifier. Particles inside the sample are visualized by a deflected laser beam and the emissions by the light scattering. These signals are processed by the microscope, enabling measurements of particle size and concentration (Kim, Ng, Bernt, & Cho, 2019).

NTA measures particles in a liquid suspension. Since the samples were already dissolved in PBS by the isolation, PBS was also used for further dilution. This was necessary for all samples after ultrafiltration. The optimal dilution ratio varied among samples due to varying amounts of particles in different SEC fractions. Accordingly, there were samples that were diluted only 1:50 with PBS, while others were diluted with 1:1000 (e.g., protein fractions). For most of the samples, however, a dilution of 1:500 with PBS proved successful. In this work, a NanoSight LM 10 instrument with the NTA 3.0. software was used. Recording time was set to 30 seconds and each sample was measured 10 times for representative measurement results. Analysis was furthermore performed with standard measurements and under temperature control.

Particle size was detected to evaluate the efficiency of particle separation, expecting the elution of large particles first, followed by smaller ones. Secondly, particle concentration per fraction was measured to determine the fractions with the highest particle yield. Analysis was performed on SEC fractions of bile and serum.

4.2.4. Transmission electron microscopy

To identify the nanoparticles as EVs, we used TEM from 10 µL thawed EV sample using negative staining technology. Negative staining was used, since unlike after isolation via UC, fractions of SEC are soluble and do not form a pellet. Thus, conventional TEM with paraffin-embedded samples was not feasible. Negative staining works by embedding biological particles in a thin layer of heavy metal salts (e.g., uranyl-acetate) and adsorbing them on a coal grid which is then analyzed under a transmission electron microscope. Thereby, it allows distinguishing of particles through morphology and specific measurements of particle size (Vergauwen et al., 2017).

Different SEC fractions, stored under different conditions were analyzed to determine the optimal specimen handling (Tab. 3).

Table 3: Overview over different sample sizes and processing conditions before TEM analysis.

Sample number	Initial SEC isolation material and volume	SEC fraction after void elution	Storage before analysis
S5	2 mL native bile	EV1+2	-80°C
S10	1 mL native bile	EV1+2	-20°C
S10	1 mL native bile	EV3+4	-20°C
S16	1 mL bile diluted with 1 mL fPBS	EV1-4	-20°C
S20	1 mL bile diluted with 1 mL fPBS	EV2	4°C over night

The negative staining solution was prepared by 4% uranyl acetate solution in dH_2O. Vortexing and sonification was done until uranyl acetate was dissolved completely, followed by centrifugation for 15 minutes at 13,000g.

In the meantime, the coal grid was prepared by placing it facing up on a microscope slide in a glow discharge unit, where it was treated for a minimum of 30 s at 10 mA.

For the straining process the grid was placed on the 10 µL sample for 10 minutes (grid on drop), dried on Whatman Paper and washed two times in drops of dH_2O by dipping the grid on the drop and drying again on Whatman Paper. Directly afterwards the grid was placed for 3 seconds on 20 µL of pre-prepared Staining Solution. Lastly the grid was dried for 5 minutes in the tweezer facing down.

Examination under the electron microscope was kindly performed by Carola Schneider of the Heinrich Pette Institute.

4.2.5. Protein concentration

Proteins were isolated from bile-derived SEC fractions by adding protein lysis buffer to the sample in a 1:4 concentration and sonification, followed by centrifugation for 25 minutes at 11,000 g at 4°C. The lipid-containing pellet was discarded, and the supernatant was used for protein concentration analysis, performed with

bicinchoninic acid assay (BCA assay, ThermoFisher). For this, 10 µL samples were pipetted into a 98 well plate next to the standard simulated by BCA and H_2O. Measurement was done in duplicates. 200 µL reaction mixture (BCA-reagent A:BCA-reagent B in the ratio of 50:1) was added to samples and standards, followed by 30 minutes incubation time at 37°C while sealed with a cap. Afterwards protein concentration was measured with Elisa Reader at 380 nm.

4.3. MicroRNA

4.3.1. MiRNA-isolation

After confirmation of the presence of EVs in the eluted fractions after SEC, miRNA was isolated from the EV zone of bile samples and cell free bile from 9 patients.

MiRNA-isolation from the EV fractions was performed using miRNeasy columns (Qiagen) following the instructions from the manual. Isolation from 300 µL native bile, drawn from the same patients at the same time as the bile used for EV isolation, followed a modified protocol by Yan et al. for native bile in a small sample size (2018). Here, TRIzol Lysis Reagent was added to the sample, mixed by vortexing and incubated for 5 minutes. Next, chloroform was added, mixed by vigorously shaking and incubated for 3 minutes afterwards. Then samples were centrifuged at 11,000 g for 15 minutes at 4°C for phase separation. The upper aqueous phase was transferred to a new microcentrifuge tube and ethanol was added and mixed by pipetting. Subsequently 700 µL of the sample was transferred to a RNeasy Micro Column and centrifuged at 8,000 g for 15 seconds at room temperature. The flowthrough got discarded and the rest of the sample was applied to the same column and centrifuged as before. Then two washing steps with buffer RPE followed, centrifuged at 8,000 g for 15 seconds and 2 minutes, respectively. The flowthrough was discarded each time. Membrane drying was conducted by centrifugation at 8,000 g for 1 minute. Afterwards the column was transferred on to a 1.5 mL microcentrifuge tube and 30 µL RNase free water (preheated to 55°C) was applied directly onto the membrane, eluting miRNA by centrifugation at 8,000 g for 1 minute. Eluted miRNA was stored on ice for downstream analysis and at -80°C for long term storage.

For quantitative Analysis of miRNA content, we used Qubit miRNA Assay Kit (ThermoFisher). Samples were then stored at -80°C until analysis with Taqman Micro Assay for miR-1281, 640 and 412 (ThermoFisher).

4.3.2. MiRNA RT-PCR

For Real Time quantitative PCR analysis, EV-derived miRNA was isolated as previously described and afterwards transcribed into cDNA. For this, we used High-Capacity cDNA Reverse Transcriptase Kit (ThermoFisher). All reactions were performed on ice.

First, a mastermix was prepared, containing:

- 1.5 µL 10x RT Buffer
- 1 µL multiscribe RT
- 4.16 µL RNase free water per reaction

Secondly, 3 µL of RT-primer was added, followed by 5 µL of RNA sample, adding to a reaction volume of 15 µL. The solution was mixed gently and centrifuged briefly, then incubated for 5 minutes on ice before inserting into a ThermoCycler.

The Thermocycler was programmed as followed:

30 minutes at 16°C

30 minutes at 42°C

5 minutes at 5°C

Stored at 4°C

Obtained cDNA was then used for Real Time quantitative PCR. For one reaction 7.76 µL RNase free water was added to 10 µL TaqMan 2x Universal Mastermix, followed by 1 µL TaqMan MicroRNA Assay probe (20x) and 1.33 µL cDNA, adding up to a sample volume of 20 µL. Every sample reaction was performed fourfold for validation and additionally 10% of reagent volumes was added standard volute to prevent pipetting loss.

The qPCR was programmed via ViiA 7 software as followed:

Setup experiment:

96 well plate 0.1 mL

Comparing ct delta delta

TaqMan

Standard properties (not fast)

Define:

Reference sample: H_2O (N)

Endogenous control: multiple

ROX control

Run method:

Sample volume 20 µL

Heat: 10 minutes at 95°C, 40 cycles (15 seconds 95°C + 60 seconds 60°C)

4.4. Statistical analysis

The statistical evaluation was carried out using the program R. Non-parametric tests Mann-Whitney U-test for 2 groups and Kruskal-Wallis-test for >2 groups were used. *P*-values less than 0.05 were regarded as statistically significant.

5. Results

To investigate whether bile-derived EVs serve as potential biomarkers in a prospective study for the distinction of biliary stenoses, we have first tested SEC on the bile of patients undergoing ERC with indeterminate biliary stenosis. Second, we evaluated miRNA content of EVs as well as the protein fraction after SEC for feasibility as potential biomarkers.

5.1. Elution profiles of bile and serum during SEC

SEC has previously shown to be feasible for EV isolation in various body fluids, however to our knowledge not yet in bile specimen (Bao et al., 2022). Therefore, we

used a stepwise approach, firstly testing the feasibility of the iZon qEV2 SEC columns by analyzing the elution profile of EVs by nanoparticle size and -concentration via NTA. Since NTA is not able to distinguish between EVs and proteins or other sample components, the term “nanoparticle” is used for all particles found in NTA analysis.

This was done to primary identify the fractions with highest concentration of EV-typical sized particles and lowest protein contamination which then could be used for further analysis. Since the used qEV2 columns were already approved for serum samples, we used serum samples of the same patients as controls.

5.1.1. Particle size

Firstly, the size of nanoparticles in the isolated fractions of both samples was measured (Fig. 9). Importantly, diluted bile (1:1 with filtered PBS) was used for EV isolation, aiming to decrease its natural high viscosity, and enabling a better flow through the column.

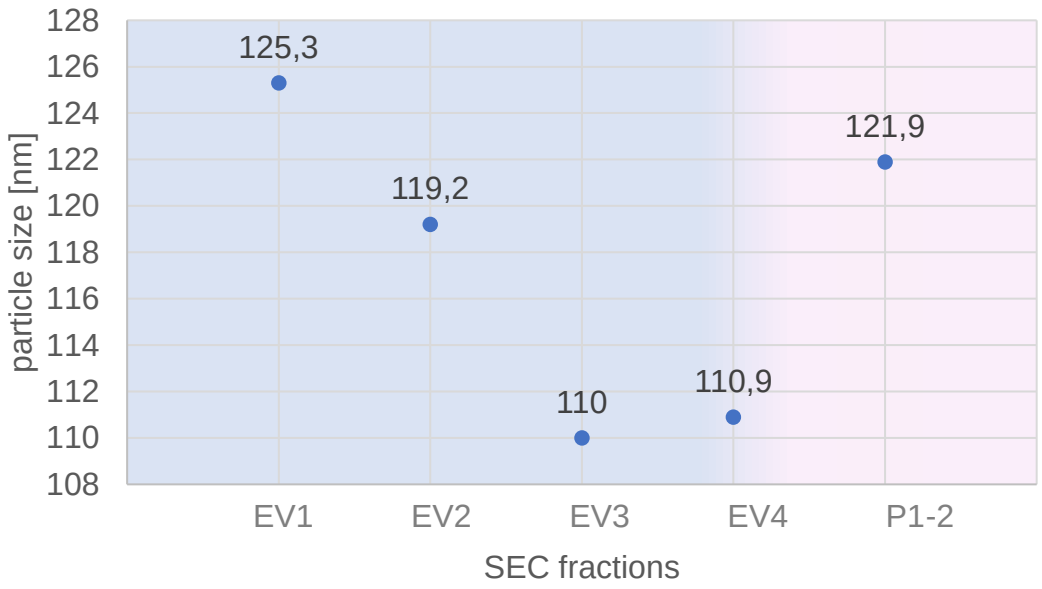

8A

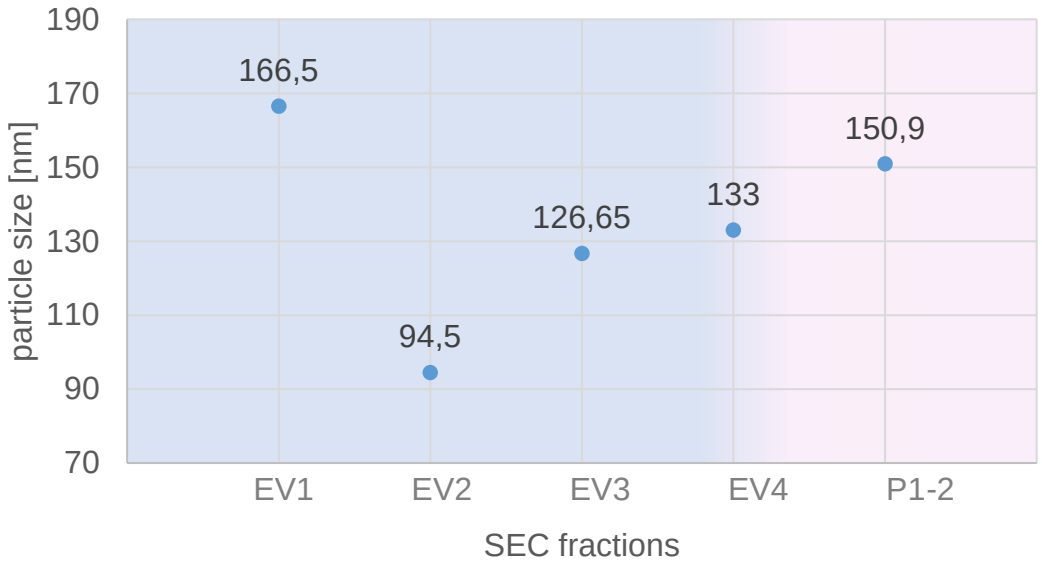

8B

Figure 9: Results of NTA measurement regarding particle size in both serum (9A) and bile (9B) samples. Importantly, the EV zone as defined by the manufacturer is marked in blue whereas the protein zone is tainted pink. **(9A)** Particle size in serum samples (n= 2) ranged from a median size of 166.5 nm (IQR: 164.3; 168.7) and 94.5 nm in fractions EV1 and EV2, respectively to 126.65 nm (IQR: 124.57; 128.72) and 133 nm (IQR: 121.2; 144.8) in EV3 and EV4, respectively. **(9B)** EV fraction of the bile sample (n= 1) showed an elution of slightly larger particles than typical EV-size (80-100 nm) in all fractions, namely 125.3 and 119.2 nm in EV1 and 2, respectively and 110 and 110.9 nm in EV3 and EV4, respectively. In protein fraction 1 (P1-2), size increased again. *SEC= size exclusion chromatography, NTA= nanoparticle tracking analysis, IQR= interquartile range, EV= extracellular vesicle*

All in all, bile and serum samples displayed a similar elution profile in terms of particle size (larger in first and last fractions, smaller in second and third). However, SEC fractions from serum samples eluted larger particles compared to bile. Both samples displayed two factions within the typical EV size (80-110 nm).

5.1.2. Particle concentration

Secondly, particle concentration was measured to see in which quantity nanoparticles eluted in the EV zone and the first protein fraction. Here again SEC fractions from bile were compared to serum samples (Fig. 10).

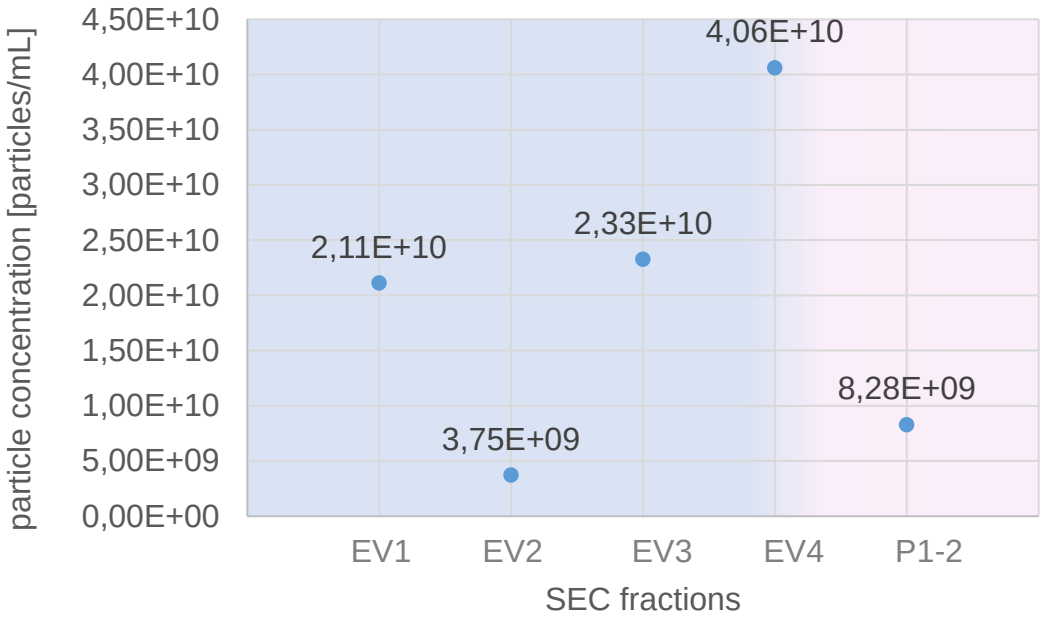

10A

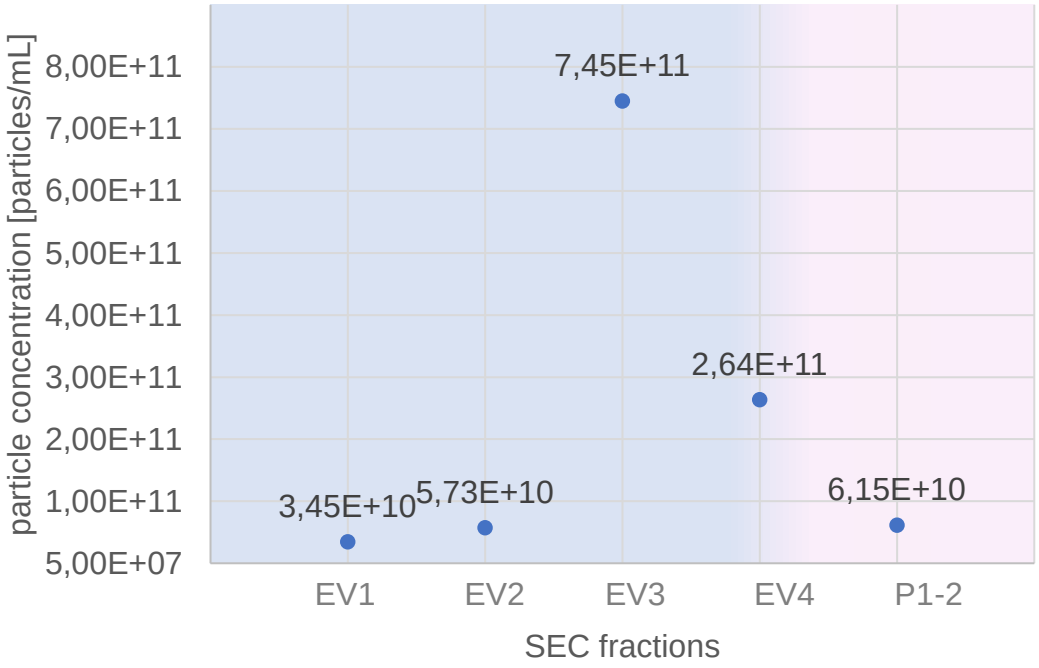

10B

Figure 10: NTA measurements for total particle concentration in serum (10A) and bile (10B) samples. EV zone is marked blue and protein zone pink. **(10A)** Serum samples (n= 2) and had a median concentration of 2,11E+10 (IQR: 1,29E+10; 2,94E+10) and 3,75E+09 (IQR: 3,75E+09; 3,75E+09) particles per mL in fractions EV1 and 2, respectively and displayed a peak up to median 2,33E+10 (IQR: 1,97E+10; 2,69E+10) particles per mL in EV3, before decreasing to 4,06E+10 (IQR:

2,97E+10; 5,15E+10) in EV4. **(10B)** Fractions of bile sample (n= 1) showed a steady increase of particle concentration in fractions EV1 to EV3 with a median particle concentration of 3,45E+10, 5,73E+10, and 7,45E+11 particles per mL, respectively and a peak in EV4 with a median concentration of 2,64E+11 particles per mL. *NTA= nanoparticle tracking analysis, SEC= size exclusion chromatography, EVs= extracellular vesicles, IQR= interquartile range*

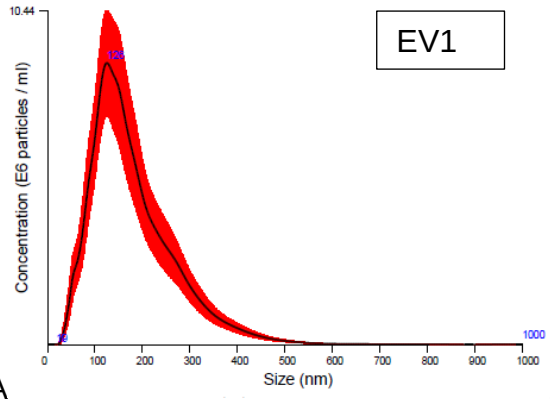

10A

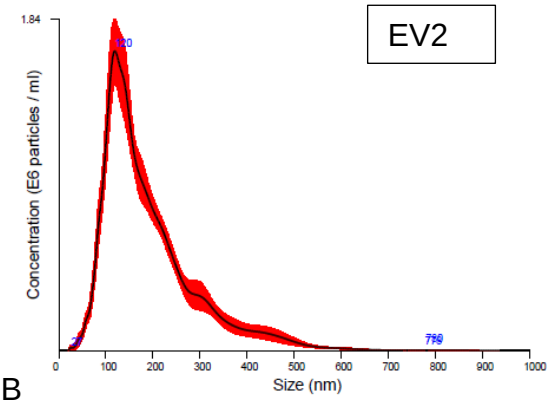

10B

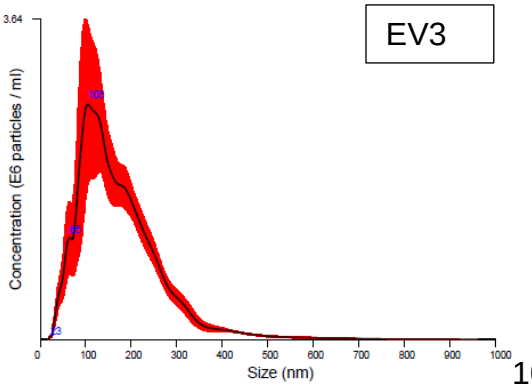

10C

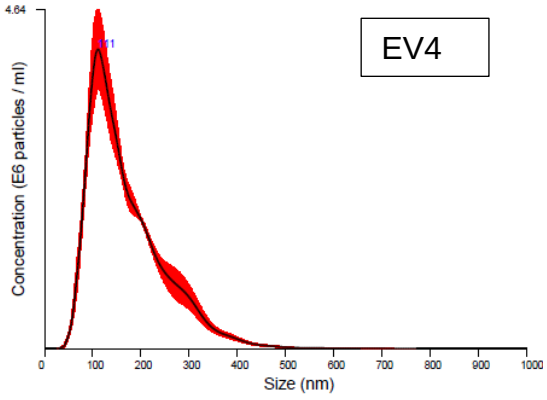

10D

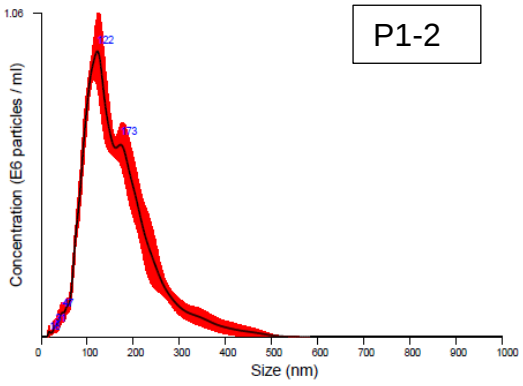

10E

Figure 11: Results of NTA measurement regarding particle size and concentration in bile sample (n= 1) as depicted by the NTA software. The graphs show a single peak in fractions EV1 to EV4 **(11A-D)** and the spectrum of particle size increases in the following protein fraction (P1-2) **(11E)** after, displaying a second peak at 173 nm. However, the range of sizes of particles with the highest concentration is relatively broad, around 100-200 nm even in the EV fractions. *NTA= nanoparticle tracking analysis, EV= extracellular vesicle*

Overall, all samples tested showed the typical Brownian motion during NTA and a slightly larger size than the typical EV-size (80-100 nm). Additionally, a higher particle concentration in bile samples compared to serum samples was observed.

5.1.3. Protein concentration

One benefit of SEC is reported to be the fewer contamination with proteins of samples. To verify this and to estimate which of the previous measured nanoparticles were proteins, protein concentration in SEC fractions from bile was measured via BCA-assays (Fig. 12). Since proteins were ought to elute late according to the manufacturer's manual, more fractions were collected and analyzed to identify the peak in protein elution.

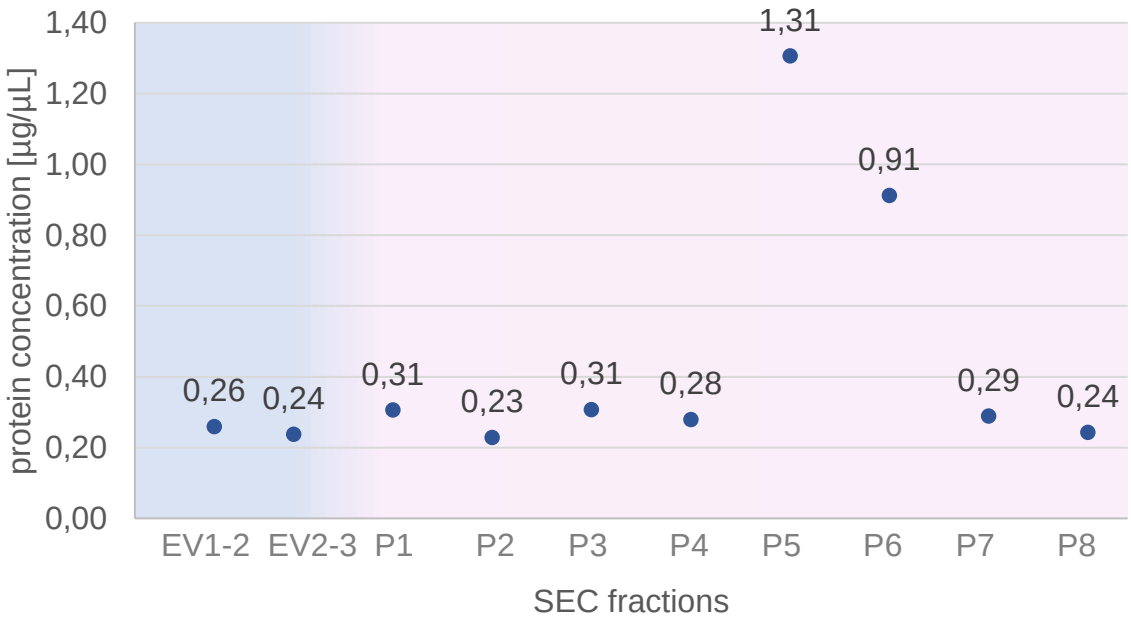

Figure 12: BCA assay results of median protein concentration in SEC fractions of bile samples. The EV zone is marked blue, whereas the protein zone is highlighted in pink. Median protein concentration in the fractions EV1 to EV4 ranged from 0.26 (IQR: 0,15; 0,37) to 0.24 (IQR: 0,21; 0,27) µg/µL and from 0.23 (IQR: 0,23; 0,23) to 1.81 (IQR: 1,17; 1,45) µg/µL in the protein zone. A peak with a median concentration of 1.31 µg/µL was noted in fraction P5. *BCA= bicinchoninic acid, SEC= size exclusion chromatography, EV= extracellular vesicle*

In order to see whether SEC was also able to separate the proteins accurately in their size, SDS-Page was performed on later fractions. This was done to estimate the feasibility of SEC-protein fractions for proteomic analysis, since proteomic analysis requires a sufficient separation for large proteins not interfering with smaller proteins.

Figure 13 shows a high protein expression in SEC fractions 33 mL after void elution (P5) and 38 mL after void elution (P6) of bile samples (n= 2) after Coomassie Staining and Ponceau Staining. Although smaller sized proteins (55kDa, 40kDa and 30kDa) were detectable in P5 and P6 as well, SEC did not show the desired separation since there was also a high abundance of large proteins (70kDa) in these fractions.

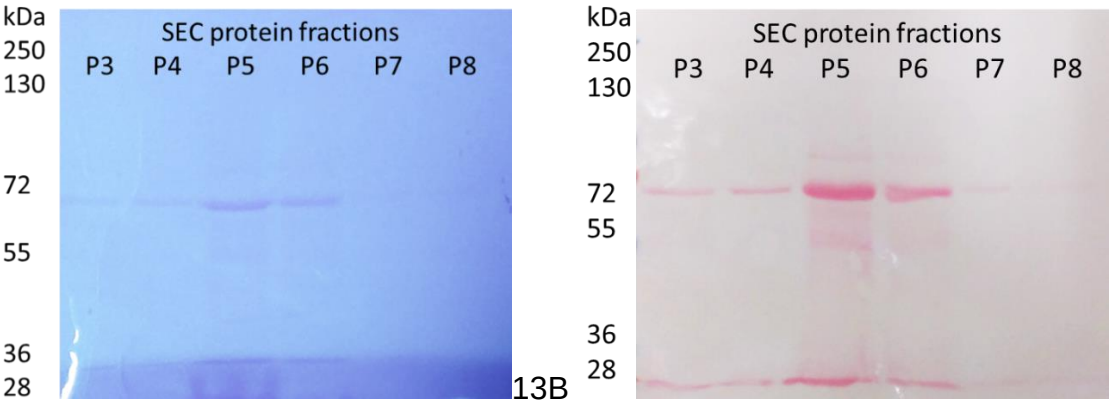

Figure 13: Characterization of protein elution during SEC of 1 mL bile by SDS-PAGE (13A) and Coomassie staining (13B). (13A) SDS-PAGE after Coomassie staining **(13B)** and the blotted membrane after Ponceau Staining of SEC fractions of bile samples (n= 2) showing large (70 kDa) protein content in all fractions with a peak in fractions P5 and 6. *SDS-PAGE= sodium dodecyl sulfate polyacrylamide gel electrophoresis, SEC= size exclusion chromatography*

5.2. Extracellular vesicles

After a first analysis of the eluted particles by NTA, bile samples were verified for the presence of EVs. Gold standard of EV verification included the evidence of typical size in NTA, the detection of EV typical markers via immunoblotting, and direct imaging with TEM to evaluate the morphology of particles.

5.2.1. Immunoblotting

In order to prove presence of EVs in the EV fractions from bile samples after SEC, surface proteins were detected using immunoblotting with protein markers CD9 (successful in 4/6) and TSG101 (4/7). Results are depicted in Figure 14.

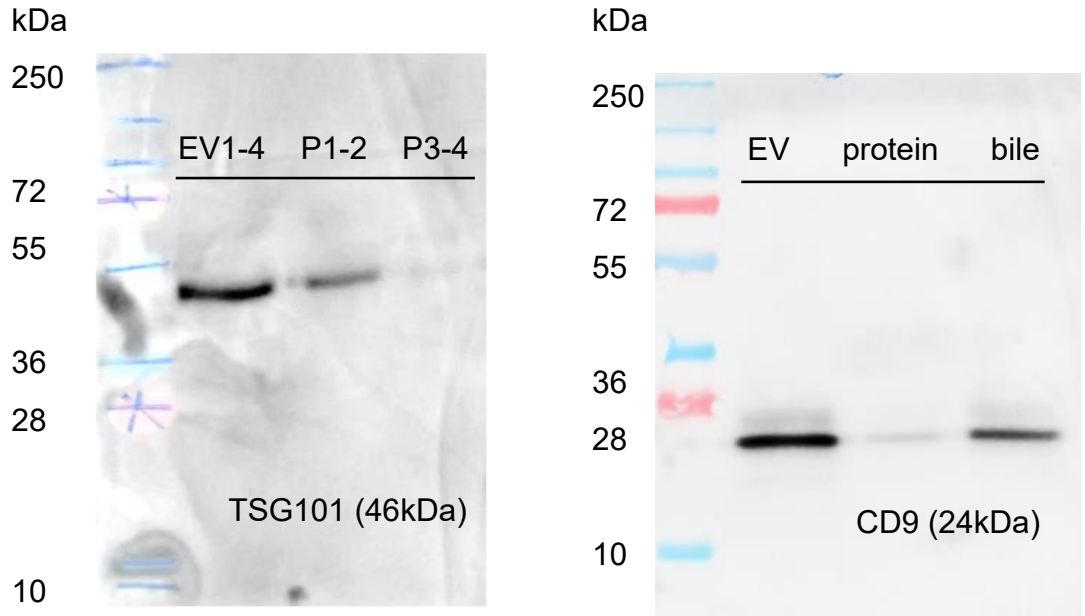

14A 14B

Figure 14: Immunoblotting of EV samples. (14A) Expression of TSG101 in the EV fractions (EV1-4) and protein fractions (P1-2 and P3-4) of 1mL bile sample. TSG101 size of 46 kDa matched the location of the highlighted band. The signal appears strongest in the EV fraction, decreasing in P1-2 and is barely visible in P3-4. **(14B)** Expression of CD9 in SEC fractions of 1mL bile diluted with 1 mL filtered PBS (1:1). Analyzed were the EV1-4 and P1-2 compared with cell free bile. CD9 displayed a high signal in the EV fraction at the expected height of 24 kDa. No expression was found in P1-2 nor P3-4. Interestingly, also cell free bile showed expression of CD9. *EV= extracellular vesicle, SEC= size exclusion chromatography*

All in all, immunoblot analysis gave strong evidence for the presence of EVs in the EV zone.

5.2.2. Transmission electron microscopy

As a final proof of the presence of EVs in bile after SEC, TEM was performed of SEC fractions (n= 5) from native or diluted bile of three different conditions (fresh isolation, stored at -20°C and at -80°C after isolation).

Images 5.7 (A-D) show TEM pictures of the SEC fractions of bile samples. All TEM images show EV-typical particles.

15A 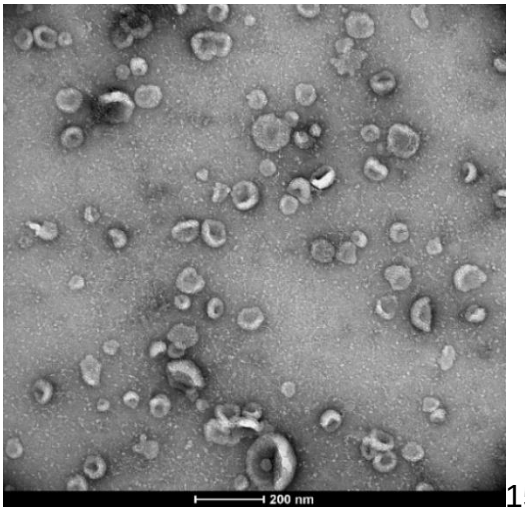

15B 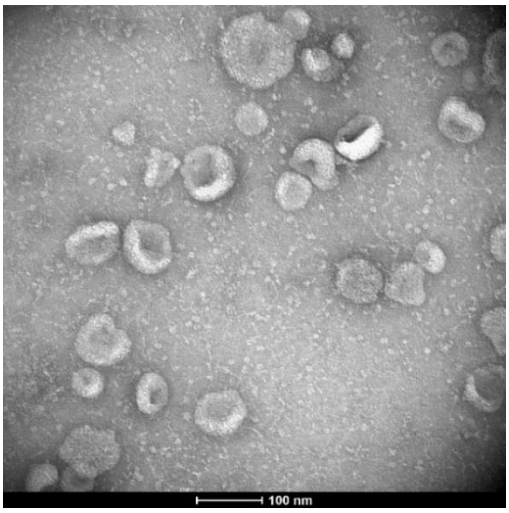

15C 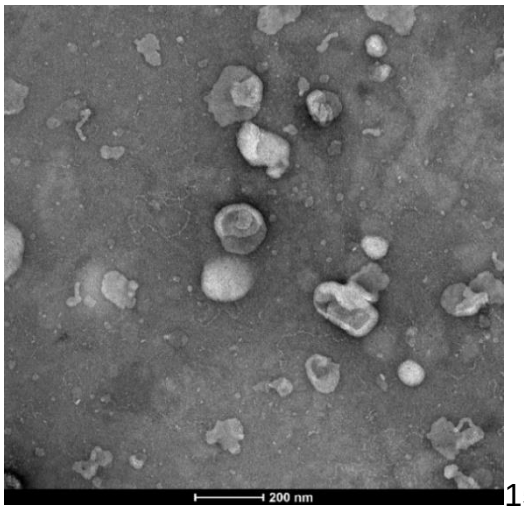

15D 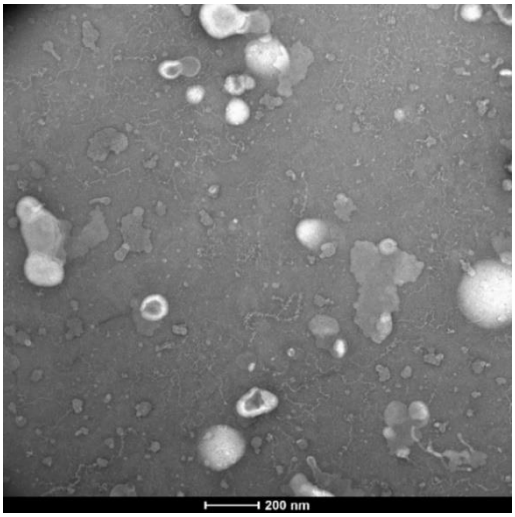

Figure 15: Visualization of EVs from bile after SEC via TEM. (15A+B) Typical rounded morphology and size (~110 nm) in the EV zone from a bile sample. Probes were stored at -20°C prior to the examination. **(15C+D)** TEM-images of SEC fraction

of bile sample after storage at -80°C. *EV= extracellular vesicle, SEC= Size exclusion chromatography, TEM= Transmission electron microscopy*

In summary, NTA, Immunoblotting and TEM give evidence for the existence of EV in the EV zone of bile samples. Also, since all experiments were carried out using pre-frozen samples, the existence and function of EVs seems not to be affected by the freezing process. However, TEM images indicate that EVs should not be stored at -80°C, showing burst morphologies suggesting EV damage.

5.3. Patient Data

After proving the existence of EVs in bile samples, a patient cohort was analyzed for abundance of miRNA markers in EVs. Since the initial aim of this study was to see if EVs in bile could also become a feasible biomarker for indeterminate biliary stenoses, nine bile samples of patients with biliary stenoses of different etiology were chosen (Tab 4).

Of the 9 patients, 3 had a malignant stenosis, caused by cholangiocarcinoma, 3 had benign stenoses with PSC and 3 had a benign-non-inflammatory disease as underlying cause for cholestasis. Median age of patients was 58 years (IQR: 52; 63) and 44% were male. All but two patients had cholestasis with elevated yGT (>36 U/L for women and >66 U/L for men) and total bilirubin (>1.1 mg/dL). An overview over the clinical data and laboratory results of each patient can be found in the Supplementary Tables 2 and 3.

Table 4: Patient characteristics including laboratory results at time of ERCP and specimen obtainment.

	Benign-non-inflammatory	**Chronic inflammatory**	**malignant**
n patients	3	3	3
Diagnosis	Anastomotic stenosis after OLT	PSC	CCA
Age [years]	58 (55;60.5)	42 (40.5;50)	73 (63;81)
Gender male	33%	66%	33%

Total bilirubin [mg/dL]	0.9 (0.65;1.95)	4.2 (2.4;11.25	2.3 (1.8;11.45)
yGT [U/L]	45 (29.5;117)	429 (277;645.5)	101 (52.5;315.5)
AST [U/L]	21 (17;83.5)	158 (111.5;176)	77 (74;95.5)
ALT [U/L]	28 (25.5;55)	153 (117;206)	106 (101;115.5)
AP [U/L]	76 (68;223)	863 (504.5;954)	405 (328.5;468.5)
CRP [mg/dL]	5 (4;6.5)	29 (16;46)	33 (19.5;35.5)

OLT= orthotopic liver transplantation, PSC= primary sclerosing cholangitis, CCA= cholangiocarcinoma, yGT= y-glutamyl transferase, AST= aspartate aminotransferase, ALT= alanine aminotransferase, AP= alkaline phosphatase, CRP= C-reactive protein, ERCP= endoscopic retrograde cholangiopancreatography

5.4. MiRNA profiles

For detection of microRNA we chose three pre-validated markers (miR-1281, miR-412 und miR-640) from previous studies.

miRNA expression profiles were measured from bile-derived EVs of 9 patients via qPCR (Fig. 16). Here, miR-412 showed a similar expression in both patients with benign (median 0.004430 (IQR: 0.004267; 0.004505)) and malignant stenoses (median 0.004407 (OQR: 0.004291; 0.004563)), but a lower abundance in patients with chronic inflammation (median 0.004127 (IQR: 0.004087; 0.004167)). However, the difference of miR-412 expression between malignant and chronic inflammatory group was not significant (*p*-value= 0.3865). miR-640 profiles, too, exhibited no significant differences in different patient cohorts (*p*-value= 0.5063). In patients with chronic inflammatory diseases, miR-1281 showed a high abundance (median 0.1147 (IQR: 0.1120; 0.1175)), whereas the expression was lower in patients with malignant stenoses (median 0.05347 (IQR: 0.04881; 0.06476)) (*p*-value= 0.1493). EVs isolated from bile of patients with benign non-inflammatory diseases showed a median miR-1281 expression of 0.07846 (IQR: 0.07625; 0.08550).

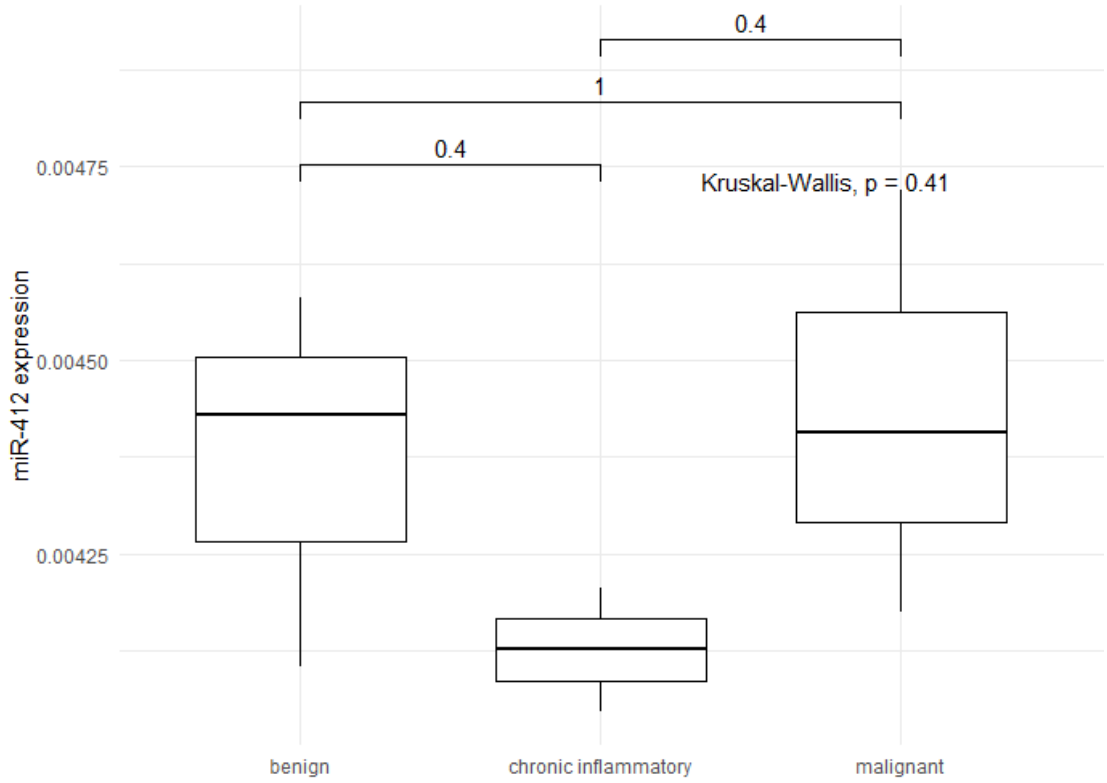
0.4
1
0.4
Kruskal-Wallis, p = 0.41
0.00475
0.00450
0.00425
miR-412 expression
benign
chronic inflammatory
malignant

16A

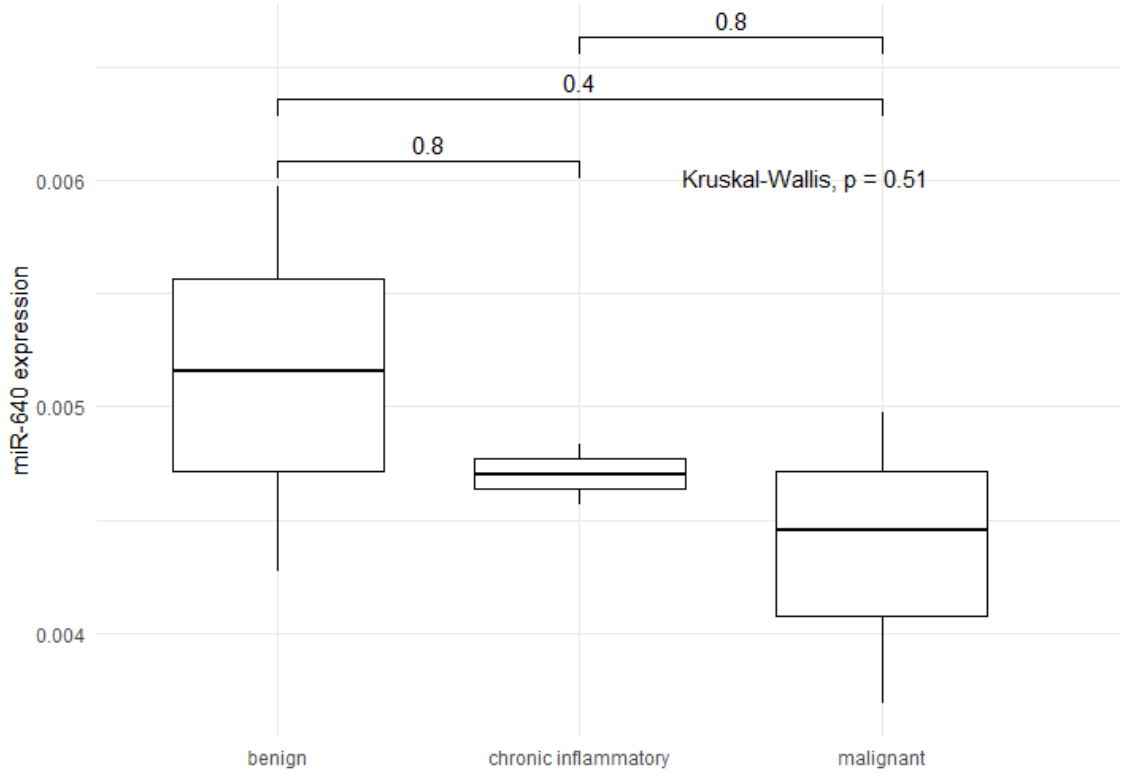
0.8
0.4
0.8
Kruskal-Wallis, p = 0.51
0.006
0.005
0.004
miR-640 expression
benign
chronic inflammatory
malignant

16B

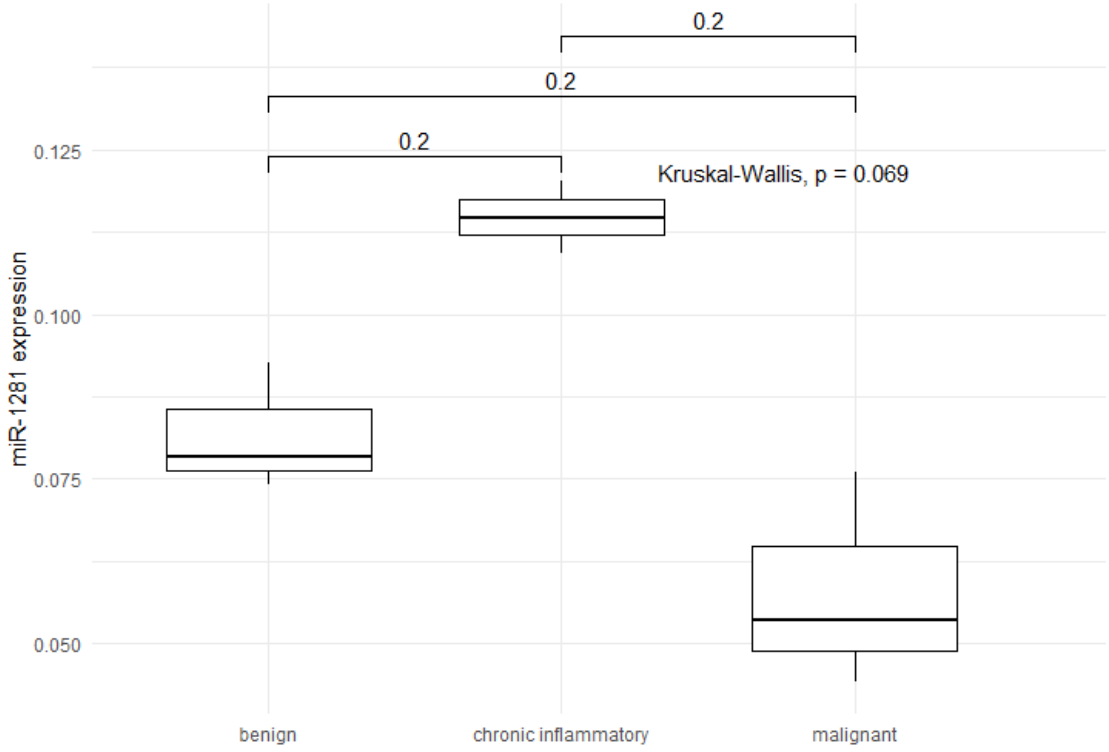

16C

Figure 16: Profiles of pre-defined miRNAs (**16A**= miR-412, **16B**= miR-640, **16C**= miR-1281) in EVs isolated from bile in patients with benign-non-inflammatory stenoses (n= 3), chronic inflammatory stenoses (n= 3), and malignant stenoses (n= 3). The tested miRNA expression in the three groups was not significantly different (*p*-values= 0.41, 0.51 and 0.069, respectively). However, miR-640 and miR-1281, which play a role in tumor suppression, displayed the expected tendency of a lower expression in patients with malignancies. *miRNA= microRNA, EVs= extracellular vesicles*

Ultimately, miRNA was isolated from cell free bile since its diagnostic potential has been previously described. Especially miR-620 and miR-412 have been found in cell free bile and displayed alterations in CCA patients compared to healthy individuals. However, in this study, only miRNA-1281 could be detected (Fig. 17). MiR-620 and miR-412 were undetectable. Similar as in EVs, miR-1281 expression in bile was found higher in the chronic inflammatory group (median 0.008270 (IQR: 0.007863; 0.008998)) than in the benign group (median 0.006455 (IQR: 0.006043; 0.006807)) (*p*-value= 0.08086). But inversely, the malignant group (median 0.007818 (IQR:

0.007488; 0.008055)) showed a higher expression than the benign group (*p*-value= 0.1904). None of these alterations was significantly different.

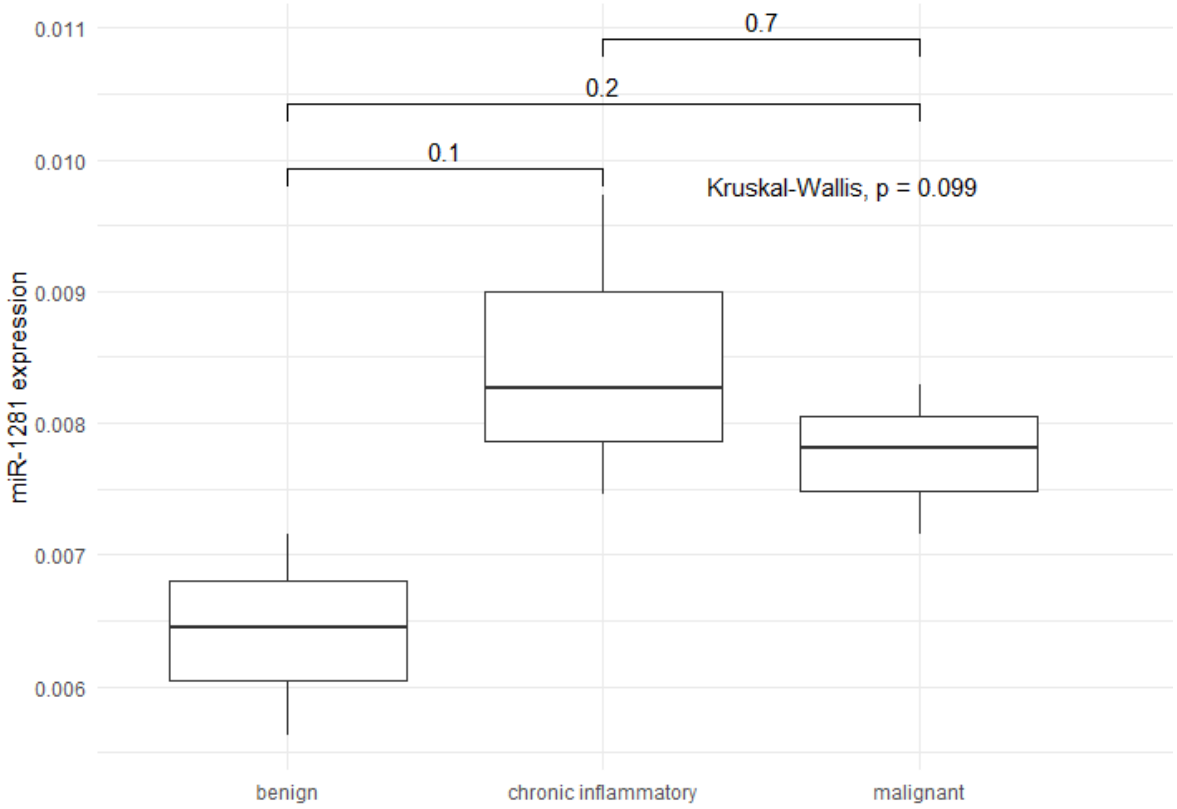

Figure 17: miRNA expression profile of miR-1281 isolated from bile of patients with benign-non-inflammatory- (n= 3), chronic inflammatory- (n= 3), and malignant stenoses (n= 3). Differences in patient cohorts showed no significant alterations (*p*-value= 0.099). Both miR-640 and miR-412 were not detectable.

All in all, miRNA expression showed a tendency toward lower abundance for tumor suppressive miRNAs such as miR-1281 and miR-640, as well as a higher abundance of oncogenic miR-412 in the malignant group.

6. Discussion

This study describes the isolation of extracellular vesicles using SEC from bile for the first time (Bao et al., 2022). We demonstrated that not only EVs can be successfully isolated by this method but can also be used to analyze distinct miRNA-patterns in patients with unclear biliary stenoses, that may serve as biomarkers in the future.

SEC was originally invented for separation of proteins, which is now increasingly used in the isolation of EVs. Due to this protective isolation process, EVs remain intact and functional, and it has also been shown that protein contamination is lower compared to ultracentrifugation (Benedikter et al., 2017). In this work, too, EVs were successfully isolated using SEC in combination with ultrafiltration, ultrafiltration being used for reducing sample sizes to about 400-500 µL.

Interestingly, a comparison of serum and bile EVs showed that EVs from bile were comparatively smaller (110 to 125.4 nm in bile samples compared to 94.5 to 170.9 nm in serum samples). The elution profiles were also slightly different, with bile eluting higher concentrations of nanoparticles than observed in serum samples. This study aimed to optimize the SEC procedure for bile samples, which was facilitated by previous centrifugation and dilution with filtered PBS, as has been done in other studies using viscous body fluids such as saliva (Aqrawi et al., 2017), seminal fluid (Rodriguez-Caro et al., 2019) or milk (Vaswani et al., 2019). Also, another study, which used bile for EV isolation via UC, inserted a dilution step to reduce viscosity (Severino et al., 2017).

The diagnostical use of bile to differentiate malignant and benign biliary stenoses seems promising, since bile has direct contact with the biliary lesion and thus a high number of potential tumor-derived EVs can be expected. A study by Han et al. found bile to represent oncogenic characteristics of extrahepatic CCA tissue samples, suggesting its high potential as a biomarker for eCCA (2020). Also, another previous study by Severino et al. found a high potential in bile-derived EVs for diagnosing CCA, measuring for EV size and concentration. The authors found the diagnostic performance of bile-derived EVs to be superior to serum-derived EVs. They hypothesized that this is because locally collected bile escapes the interferences that circulating body fluids, such as serum, are subject to (2017).

In this study, more EVs were found in bile than in serum using SEC isolation. This was observed by NTA measurements, showing a concentration ranging from 3,45E+10 to a maximum of 2,64E+11 particles per mL in the EV zone of bile, and a median concentration of 2,11E+10 (IQR: 1,29E+10; 2,94E+10), 3,75E+09 (IQR: 3,75E+09; 3,75E+09) and 2,33E+10 (IQR: 1,97E+10; 2,69E+10), and 4,06E+10 (IQR: 2,97E+10; 5,15E+10) particles per mL in the EV zone of serum samples.

Yet, the concentrations achieved by Severino et al. exceed the concentrations found in this work by far. They found nanoparticle concentrations in patients with malignancies compared to nonmalignant biliary stenoses to be 2.41E+14 vs 1.60E+14 particles per liter, respectively (2017). This is rather surprising, considering the reported higher yield of EVs isolated by SEC compared to UC in the literature (Benedikter et al., 2017; Nordin et al., 2015). Reasons for this are not unequivocally determinable but could lie in the different isolation method, bile composition or sample processing.

Qualitative analysis of EV surface markers by immunoblotting, showed a lower signal in serum samples. With an amount of 2 mL serum, only CD9 could be detected using the same protocol as fore bile-derived EVs (results not shown). However, it is important to note that no exact quantification can be inferred by immunoblotting (Witwer et al., 2013).

Severino et al. proposed NTA measurement of bile-derived EVs as a simple and valuable method for differentiating malignant from benign conditions according to their concentration (2017). However, it must be noted that there are some factors that can influence the measurement of NTA. This includes not only the viscosity of the sample and the properties of the EVs, such as size variability and refractive index but also external factors. These are for example temperature, vibrations, device settings and reference standards (Severino et al., 2017).

NTA measurements in this study showed nanoparticle sizes ranging from 110 to 125.3 nm, and a range from 94.5 to 170.9 nm in the EV zone of bile and serum samples, respectively. Similarly large differences and sizes have also been reported in other studies, characterizing EVs by NTA. Severino et al. reported sizes up to 207.3 nm in bile and EVs that ranged from 176.3 to 105.5 nm in serum samples from the same cohort (2017). Additionally, some authors recommend filtering serum samples through a 0.22 µm pore mesh before processing, which was not done in this work, suggesting a higher protein contamination (Arbelaiz et al., 2017).

Quantification of EVs by TEM was done by scale measurements. Overall, EV dimensions were 110 nm, definitely closer to the typical exosome size (80-100 nm) frequently reported in the literature (Crescitelli et al., 2013; Gyorgy et al., 2011; G. Liu

et al., 2019). Other studies, investigating EVs derived from bile, also found slightly larger particles with sizes up to 110 nm (L. Li et al., 2014; Nakashiki et al., 2021).

In general, there has long been a debate in the literature about the optimal storing temperature of pre-isolation samples and isolated EVs. Some studies found an increase in EV sizes after storage at -80°C to up to 125 ± 1.15 nm, leaving size measurements via TEM for example less conclusive (Gelibter et al., 2022; Maroto et al., 2017). But importantly, here, samples were frozen after EV isolation. Other studies which analyzed fresh EVs from previously frozen plasma samples showed no changes in EV morphology or protein content measured by mass spectrometry (Sarker et al., 2014). Another study found that EVs stored at both -20°C or -80°C displayed the same morphology and concentration as unfrozen samples but were altered in functional properties (Ramirez et al., 2018). This however contradicts to a study that tested the detectability of TSG101, a surface marker of EVs, at different times after storage at different temperatures (4°C to -80°C). It turned out that TSG101 was detectable in all samples and that EVs could still be transferred into cells, meaning the function of TSG101 as a transporter was still intact (Ramirez et al., 2018). However, no studies have measured the influence of storage conditions on the analysis of -omics, such as lipidomics, proteomics or transcriptomics, implying further need for research in this field.

In this study, all samples were stored at -80°C before EV isolation and at 4°C afterward, and the detection of surface markers on EVs was successful. Furthermore, miRNA could be isolated from EV fractions, which strongly speaks for an isolation of intact EVs. TEM imaging of isolated EVs, tentatively stored both at -20°C and -80°C showed a slightly larger size and a burst morphology of EVs, respectively. This, in synopsis with the above-mentioned studies, suggests the feasibility of freezing samples before EV isolation but not afterwards.

MiRNA analysis of bile-derived EVs revealed a trend towards lower expression of miR-1281 and miR-640 in patients with cholangiocarcinoma compared to benign biliary stenoses (*p*-values= 0.1493 and 0.8, respectively). MiR-412 on the other hand showed a tendency toward higher expression in cancer patients as expected, in comparison with patients with chronic inflammatory stenoses and malignancy (*p*-value= 0.3865).

Our findings are in line with previous studies, that had identified miR-1281 and miR-640 to bear tumor suppressive potential and were downregulated in multiple tumor types (Jiang et al., 2018; Pignot et al., 2013; Tang et al., 2021; Zhai et al., 2019) and miR-412 was suggested to have a oncogenic function by promoting tumor immune escape (Wang et al., 2020).

Other studies have tested miRNAs as diagnostic markers in unclear biliary lesions. Voigtländer et al. for example, analyzed miR-412 and miR-640 in bile of patients with PSC and PSC-CCA. They found a significant overexpression of miR-412 and downregulation of miR-640 in patients with PSC-CCA compared to PSC patients without cholangiocarcinoma. Furthermore, they calculated for the differentiation of PSC patients with and without CCA (PSC-CCA) a sensitivity of 50% (both) and specificities of 89% (miR-412) or 92% (miR-640), respectively. Additionally, they tested miR-1281 in serum of patients with PSC and CCA revealing a significantly higher expression in patients with PSC compared to CCA. A following analysis of sensitivity and specificity regarding differentiation of PSC and CCA patients showed a high specificity of 90% and lower sensitivity of 55% at a cut off value of <1,44 (2015). Further, Yan et al. observed miR-1281 in serum-derived EVs of patients with colorectal cancer being downregulated compared to healthy individuals, suggesting it feasible as diagnostic biomarker (2017).

In a study of 2015, Roest et al. suggested the use of cell-free bile for analysis of small RNA instead of EVs, arguing that 80-90% of the miRNA pool remains in the soluble fraction after ultracentrifugation and therefore the analysis of only EVs would not represent the whole RNA spectrum. They also estimated an increase in sensitivity and specificity of miRNA biomarkers if cell-free bile was used (2015). Adversely, in this work, miR-412 and miR-640 could not be detected in bile samples via qPCR. This could be due to enzymatic degradation in bile (Lapitz et al., 2018). MiR-1281 on the other hand showed higher expression in patients with malignant stenoses and chronic inflammatory diseases compared to other benign, non-inflammatory causes for cholestasis. Interestingly, these expression patterns did not mirror the expected results and the results seen in miR-1281 expression in bile-derived EVs. This seems to suggest that bile is less feasible for the analysis of - at least these three -microRNA markers, compared to bile-derived EVs.

MiRNA analysis performed in this study is subject to limitations. First, the analyzed patient cohort was small, allowing only limited extrapolations for the general population, requiring validation in a larger cohort. Second, due to the small amount of total isolated miRNA, only a restricted number of miRNA marker could be analyzed by qPCR. Basis for the selection of miRNAs was a previous study, leaving the results susceptible to selection bias. Lastly, the selection of pre-described miRNA biomarkers for PSC-CCA was difficult, since there is limited literature about EVs isolated from bile in general and even less studies performed on miRNAs isolated from bile-derived EVs (Lapitz et al., 2018). Here, a more general approach e.g., by using larger assays (Voigtlander et al., 2015) or next generation sequencing on miRNAs in bile-derived EVs would be more insightful, however the purity or amount of miRNA isolated in this study was not sufficient for this kind of analysis. Reasons therefor could be a still too high contamination with other particles in the sample, interfering with the miRNA (D. S. K. Liu et al., 2020; Stranska et al., 2018). Another possible explanation could be the degradation of miRNA during the isolation process.

Difficulties with low amounts of isolated RNA from biofluid-derived EVs have been described before, yielding concentrations below the detection limit of fluorimetry or capillary electrophoresis (Ramirez et al., 2018). A number of processing steps have been suggested to overcome this problem, e.g. normalizing fractions by the initial sample input volume used for EV isolation and, before downstream analysis, vacuum concentrating the extracted RNA (Ramirez et al., 2018).

Nevertheless, the analysis of miRNA in this study showed, that EVs, isolated via SEC were still intact after the isolation process and contained miRNAs, previously described in patients with PSC and PSC-CCA. Further, although not significant, the abundance of these markers showed a tendency as expected according to previous studies.

Ultimately protein analysis was performed. Beforehand, a similar gradient regarding protein size, such as in separation of EV and proteins was expected. This could have possibly eased a protein or even proteome analysis since larger proteins often distract signals of smaller proteins in proteomic analysis. A sufficient separation could have prevented this. Unfortunately, the expected gradient of large proteins in earlier fractions and smaller proteins in later fractions could not be observed. SEC columns

from iZON are specifically validated for EV separation and not protein separation. As already mentioned in the introduction, there are many different SEC columns available with different parameters regarding matrix and pore size (Cutler, 2004). Although protein profiles detected with SDS-PAGE seemed not very promising, proteomic analysis of both fractions containing EVs and fractions of the protein zone were given away for proteomic analysis via mass-spectrometry (data not shown). Previous studies have found a high diagnostic use of proteomics from bile (Son, Ahn, Kim, & Kim, 2020; Voigtlander et al., 2017) and EVs (Arbelaiz et al., 2017; Dutta et al., 2015; Hoshino et al., 2020) in patients with cholangiocarcinoma. Arbelaiz et al. studied serum-derived EVs isolated via UC from patients with CCA, PSC and PCA. They found several proteins analyzed via LC-MS showing high diagnostic values, for example in patient groups early staged CCA vs PSC, an AUC of 0.956 (2017).

However, proteomic analysis in this study showed no usable results. This was due to interference of large proteins in the samples.

Regarding the implementation in the clinical setting there are some limitations to consider. First, since ERC is an invasive procedure with potential life-threatening complications, indication must be put carefully and is not feasible for every patient, limiting sample collection. However, it is important to note that ERC is commonly performed for the evaluation of biliary stenoses since has both diagnostic and therapeutic value. Therefore, sample collection might not be extremely limited, additionally considering the significantly lower complication rate of ERC performed in specialist centers (Aabakken et al., 2017) and the fact that bile aspiration is considered as a relatively safe procedure (Fior-Gozlan et al., 2016).

Second, bile-derived EV isolation via SEC is a rather lengthy process with a high number of processing steps, including several centrifugation steps and fraction collection by hand. Especially the collection of fractions by hand makes an analysis of more than three samples at a time very challenging. Here, an automated sample collector might come in handy, if more samples need to be analyzed at the same time. Also, the use of smaller SEC columns with less sample capacity but also less amounts of buffer needed, could be investigated. TEM images from this study have shown a high abundance of EVs using 1 mL bile, suggesting a smaller sample size might suffice as well. Also, other studies which isolated EVs from bile mostly used

smaller sample sizes, but importantly used ultracentrifugation (L. Li, Piontek, Kumbhari, Ishida, & Selaru, 2016; Severino et al., 2017). Another option would be focusing on the purest fraction and not collecting the others. This would save time and enable the analysis of more samples at the same time. Based on the findings in this study, this would probably be the fraction containing the first 4-6 mL after void elution, since it showed most EV-typical sizes in the NTA analysis, and a high concentration compared with the other fractions. On the other hand, the low amount of miRNA yielded in this study with in an already comparatively large sample might decrease even more when using smaller sample sizes.

7. Conclusion and outlook

In order to securely distinguish the underlying etiology of patients suffering from biliary stenoses, reliable biomarkers are urgently required.

We evaluated bile-derived EVs using size exclusion chromatography, proving that, although previously not described in the literature, this method is feasible for isolation. Furthermore, our findings suggest EV-derived miRNAs as a biomarker for the distinction of biliary stenoses, which needs verification in a larger cohort study. Additionally, it would be interesting to compare EVs isolated via SEC from bile and serum, regarding their abundance and diagnostic power for biliary stenoses. This would probably give a good impression of what status and area of application could exist for EVs derived from bile in the future. Especially, since at least to-date, serum is easier to obtain in the clinical setting and there is more literature available on serum-derived EVs. However, there are indications that bile indeed may have an advantage over serum in the diagnosis of malignant biliary stenoses, as Severino et al. demonstrated in their study, analyzing bile and serum EVs using ultracentrifugation (2017).

In addition, a proteome analysis of the EVs could offer further possibilities for the differentiation of biliary stenoses, as Arbelaiz et al. have already demonstrated in serum (2017). For this, an improved isolation process must be developed to further minimize large protein contamination.

It is important to note, that this study is building the base for the analysis of a multicentered study, aiming to establish a diagnostic algorithm for patients with indeterminate biliary lesions. Indeterminate meaning that even after MRCP and ERCP no final diagnosis can be made. The diagnostic algorithm will not only include EVs from bile but other promising marker, of both proteins and nucleic acids found in previous studies to provide a full roundup of diagnostic markers to-date.

8. Abstract

Background: Biliary stenoses pose a diagnostic challenge due to the various underlying conditions of both malignant and benign etiologies. Extracellular vesicles (EVs) were shown to have predictive potential in the identification of underlying cholangiocarcinoma, and therefore have been of rising interest in the past years. Their abundance in all kinds of body fluids and their ability to enable communication between cells makes them feasible for both diagnostic and therapeutic experimental approaches. However, isolation of bile-derived EVs remains technically challenging, leaving its diagnostic potential unrevealed. **Aim:** In this study, we aimed to establish EV isolation from bile of patients with biliary stenoses, using a novel technique of size exclusion chromatography (SEC). To test their diagnostic potential, we wanted to test whether the presence of EV-derived miRNA or proteins could distinguish benign from malignant biliary stenoses. **Methods:** Bile-derived EVs were isolated via SEC and the presence of miRNA was determined. Further, we characterized proteins of later isolated fractions by SEC to test its feasibility for further proteomic analysis. **Results:** EVs could be successfully isolated from bile via SEC, presenting the typical size, morphology, and surface markers. Established miRNA markers were detected in bile-derived EVs of patients with biliary stenoses, revealing their diagnostic potential in distinguishing benign from malignant stenoses. **Conclusion:** EV isolation from bile samples was feasible with SEC. Extracted EVs contained specific miRNA which can serve as biomarkers for the differentiation of biliary stenoses in the future. Studies with larger cohorts will be needed to confirm these findings.

9. Zusammenfassung (Deutsch)

Gallengangsstenosen stellen aufgrund der verschiedenen zugrunde liegenden Erkrankungen sowohl maligner als auch benigner Ätiologie bis heute eine diagnostische Herausforderung dar. Aufgrund ihres bisher vielversprechenden experimentellen Einsatzes als Biomarker für u.a. das Cholangiokarzinom sind Extrazelluläre Vesikel (EVs) daher in den letzten Jahren von steigendem Interesse gewesen. Ihr Vorhandensein in verschiedenen Körperflüssigkeiten und ihre Fähigkeit zum Crosstalk zwischen Zellen macht sie sowohl für diagnostische als auch für therapeutische Ansätze interessant. Die Isolation von Gallen-EVs bleibt jedoch technisch schwierig, sodass ihr diagnostisches Potenzial bisher unausgeschöpft bleibt.

Ziel dieser Studie war es, die Isolation von EVs aus Galle von Patienten mit Gallengangsstenosen unter Verwendung der „Size Exclusion Chromatography“ (SEC) zu etablieren. Die SEC gilt als schneller, einfacher und sauberer als die bisher meist verwendetet Ultrazentrifugation. Um das diagnostische Potenzial weiter zu bestimmen, wollten wir testen, ob die in den EVs befindliche miRNAs oder Proteine benigne von malignen Gallenstenosen unterscheiden können.

Hierfür wurden EVs mittels SEC aus der Galle von Patienten mit PSC, CCA und Z.n. LTX isoliert und mittels Immunoblotting, Transmission Elektronmikroskopie und Nanoparticle Tracking Analysis charakterisiert. Anschließend wurden die EV-Fraktionen auf miRNA Marker getestet. Außerdem wurde die Proteinfraktion charakterisiert, um ihr Potential für eine Proteomanalyse einschätzen zu können.

Insgesamt, konnten mittels SEC erfolgreich EVs aus Galle isoliert werden, mit Nachweis der typischen Größe, Morphologie und Oberflächenmarker. Des Weiteren konnten etablierte miRNA-Marker in den EVs nachgewiesen werden, was ein diagnostisches Potenzial bei der Differenzierung von unklaren Gallengansstenosen vermuten lässt.

10. References

Aabakken, L., Karlsen, T. H., Albert, J., Arvanitakis, M., Chazouilleres, O., Dumonceau, J. M., . . . Hassan, C. (2017). Role of endoscopy in primary sclerosing cholangitis: European Society of Gastrointestinal Endoscopy (ESGE) and European Association for the Study of the Liver (EASL) Clinical Guideline. *Endoscopy, 49*(6), 588-608. doi:10.1055/s-0043-107029

Abou-Alfa, G. K., Sahai, V., Hollebecque, A., Vaccaro, G., Melisi, D., Al-Rajabi, R., . . . Vogel, A. (2020). Pemigatinib for previously treated, locally advanced or metastatic cholangiocarcinoma: a multicentre, open-label, phase 2 study. *Lancet Oncol, 21*(5), 671-684. doi:10.1016/S1470-2045(20)30109-1

Altman, A., & Zangan, S. M. (2016). Benign Biliary Strictures. *Semin Intervent Radiol, 33*(4), 297-306. doi:10.1055/s-0036-1592325

Aqrawi, L. A., Galtung, H. K., Vestad, B., Ovstebo, R., Thiede, B., Rusthen, S., . . . Jensen, J. L. (2017). Identification of potential saliva and tear biomarkers in primary Sjogren's syndrome, utilising the extraction of extracellular vesicles and proteomics analysis. *Arthritis Res Ther, 19*(1), 14. doi:10.1186/s13075-017-1228-x

Arbelaiz, A., Azkargorta, M., Krawczyk, M., Santos-Laso, A., Lapitz, A., Perugorria, M. J., . . . Banales, J. M. (2017). Serum extracellular vesicles contain protein biomarkers for primary sclerosing cholangitis and cholangiocarcinoma. *Hepatology, 66*(4), 1125-1143. doi:10.1002/hep.29291

Bao, F., Liu, J., Chen, H., Miao, L., Xu, Z., & Zhang, G. (2022). Diagnosis Biomarkers of Cholangiocarcinoma in Human Bile: An Evidence-Based Study. *Cancers (Basel), 14*(16). doi:10.3390/cancers14163921

Benedikter, B. J., Bouwman, F. G., Vajen, T., Heinzmann, A. C. A., Grauls, G., Mariman, E. C., . . . Stassen, F. R. M. (2017). Ultrafiltration combined with size exclusion chromatography efficiently isolates extracellular vesicles from cell culture media for compositional and functional studies. *Sci Rep, 7*(1), 15297. doi:10.1038/s41598-017-15717-7

Bergquist, A., Weismuller, T. J., Levy, C., Rupp, C., Joshi, D., Nayagam, J. S., . . . International, P. S. C. S. G. (2023). Impact on follow-up strategies in patients with primary sclerosing cholangitis. *Liver Int, 43*(1), 127-138. doi:10.1111/liv.15286

Bernuzzi, F., Marabita, F., Lleo, A., Carbone, M., Mirolo, M., Marzioni, M., . . . Invernizzi, P. (2016). Serum microRNAs as novel biomarkers for primary sclerosing cholangitis and cholangiocarcinoma. *Clin Exp Immunol, 185*(1), 61-71. doi:10.1111/cei.12776

Blechacz, B. (2017). Cholangiocarcinoma: Current Knowledge and New Developments. *Gut Liver, 11*(1), 13-26. doi:10.5009/gnl15568

Bowlus, C. L., Arrive, L., Bergquist, A., Deneau, M., Forman, L., Ilyas, S. I., . . . Assis, D. N. (2023). AASLD practice guidance on primary sclerosing cholangitis and cholangiocarcinoma. *Hepatology, 77*(2), 659-702. doi:10.1002/hep.32771

Bowlus, C. L., Lim, J. K., & Lindor, K. D. (2019). AGA Clinical Practice Update on Surveillance for Hepatobiliary Cancers in Patients With Primary Sclerosing Cholangitis: Expert Review. *Clin Gastroenterol Hepatol, 17*(12), 2416-2422. doi:10.1016/j.cgh.2019.07.011

Bowlus, C. L., Olson, K. A., & Gershwin, M. E. (2016). Evaluation of indeterminate biliary strictures. *Nat Rev Gastroenterol Hepatol, 13*(1), 28-37. doi:10.1038/nrgastro.2015.182

Catanzaro, E., Gringeri, E., Burra, P., & Gambato, M. (2023). Primary Sclerosing Cholangitis-Associated Cholangiocarcinoma: From Pathogenesis to Diagnostic and Surveillance Strategies. *Cancers (Basel), 15*(20). doi:10.3390/cancers15204947

Chapman, M. H., Thorburn, D., Hirschfield, G. M., Webster, G. G. J., Rushbrook, S. M., Alexander, G., . . . Pereira, S. P. (2019). British Society of Gastroenterology and UK-PSC guidelines for the diagnosis and management of primary sclerosing cholangitis. *Gut, 68*(8), 1356-1378. doi:10.1136/gutjnl-2018-317993

Chapman, R., Fevery, J., Kalloo, A., Nagorney, D. M., Boberg, K. M., Shneider, B., . . . American Association for the Study of Liver, D. (2010). Diagnosis and management of primary sclerosing cholangitis. *Hepatology, 51*(2), 660-678. doi:10.1002/hep.23294

Charatcharoenwitthaya, P., Enders, F. B., Halling, K. C., & Lindor, K. D. (2008). Utility of serum tumor markers, imaging, and biliary cytology for detecting cholangiocarcinoma in primary sclerosing cholangitis. *Hepatology, 48*(4), 1106-1117. doi:10.1002/hep.22441

Choi, D. S., Kim, D. K., Kim, Y. K., & Gho, Y. S. (2015). Proteomics of extracellular vesicles: Exosomes and ectosomes. *Mass Spectrom Rev, 34*(4), 474-490. doi:10.1002/mas.21420

Colombo, M., Raposo, G., & Thery, C. (2014). Biogenesis, secretion, and intercellular interactions of exosomes and other extracellular vesicles. *Annu Rev Cell Dev Biol, 30*, 255-289. doi:10.1146/annurev-cellbio-101512-122326

Coumans, F. A. W., Brisson, A. R., Buzas, E. I., Dignat-George, F., Drees, E. E. E., El-Andaloussi, S., . . . Nieuwland, R. (2017). Methodological Guidelines to Study Extracellular Vesicles. *Circ Res, 120*(10), 1632-1648. doi:10.1161/CIRCRESAHA.117.309417

Crescitelli, R., Lasser, C., Szabo, T. G., Kittel, A., Eldh, M., Dianzani, I., . . . Lotvall, J. (2013). Distinct RNA profiles in subpopulations of extracellular vesicles: apoptotic bodies, microvesicles and exosomes. *J Extracell Vesicles, 2*. doi:10.3402/jev.v2i0.20677

Cutler, P. (2004). Size-exclusion chromatography. *Methods Mol Biol, 244*, 239-252. doi:10.1385/1-59259-655-x:239

Deng, M., Li, S., Wang, Q., Zhao, R., Zou, J., Lin, W., . . . Guo, R. (2022). Real-world outcomes of patients with advanced intrahepatic cholangiocarcinoma treated with programmed cell death protein-1-targeted immunotherapy. *Ann Med, 54*(1), 803-811. doi:10.1080/07853890.2022.2048416

Dutta, S., Reamtong, O., Panvongsa, W., Kitdumrongthum, S., Janpipatkul, K., Sangvanich, P., . . . Chairoungdua, A. (2015). Proteomics profiling of cholangiocarcinoma exosomes: A potential role of oncogenic protein transferring in cancer progression. *Biochim Biophys Acta, 1852*(9), 1989-1999. doi:10.1016/j.bbadis.2015.06.024

Ehlken, H., & Schramm, C. (2015). How Should Cancer Surveillance in Primary Sclerosing Cholangitis Be Performed? *Viszeralmedizin, 31*(3), 173-177. doi:10.1159/000431350

Fior-Gozlan, M., Giovannini, D., Rabeyrin, M., Mc Leer-Florin, A., Laverriere, M. H., & Bichard, P. (2016). Monocentric study of bile aspiration associated with biliary brushing performed during endoscopic retrograde cholangiopancreatography in 239 patients with symptomatic biliary stricture. *Cancer Cytopathol, 124*(5), 330-339. doi:10.1002/cncy.21667

Forner, A., Vidili, G., Rengo, M., Bujanda, L., Ponz-Sarvise, M., & Lamarca, A. (2019). Clinical presentation, diagnosis and staging of cholangiocarcinoma. *Liver Int, 39 Suppl 1*, 98-107. doi:10.1111/liv.14086

Gai, C., Camussi, F., Broccoletti, R., Gambino, A., Cabras, M., Molinaro, L., . . . Arduino, P. G. (2018). Salivary extracellular vesicle-associated miRNAs as potential biomarkers in oral squamous cell carcinoma. *BMC Cancer, 18*(1), 439. doi:10.1186/s12885-018-4364-z

Gao, W., Shen, H., Liu, L., Xu, J., Xu, J., & Shu, Y. (2011). MiR-21 overexpression in human primary squamous cell lung carcinoma is associated with poor patient prognosis. *J Cancer Res Clin Oncol, 137*(4), 557-566. doi:10.1007/s00432-010-0918-4

Garzon, R., Marcucci, G., & Croce, C. M. (2010). Targeting microRNAs in cancer: rationale, strategies and challenges. *Nat Rev Drug Discov, 9*(10), 775-789. doi:10.1038/nrd3179

Gelibter, S., Marostica, G., Mandelli, A., Siciliani, S., Podini, P., Finardi, A., & Furlan, R. (2022). The impact of storage on extracellular vesicles: A systematic study. *J Extracell Vesicles, 11*(2), e12162. doi:10.1002/jev2.12162

Gradilone, S. A. (2017). Extracellular vesicles as therapeutic carriers of microRNAs for cholangiocarcinoma. *Hepatology, 65*(2), 404-406. doi:10.1002/hep.28925

Grimsrud, M. M., & Folseraas, T. (2019). Pathogenesis, diagnosis and treatment of premalignant and malignant stages of cholangiocarcinoma in primary sclerosing cholangitis. *Liver Int, 39*(12), 2230-2237. doi:10.1111/liv.14180

Guerra, I., Bujanda, L., Castro, J., Merino, O., Tosca, J., Camps, B., . . . Spanish, G. g. (2019). Clinical Characteristics, Associated Malignancies and Management of Primary Sclerosing Cholangitis in Inflammatory Bowel Disease Patients: A Multicentre Retrospective Cohort Study. *J Crohns Colitis, 13*(12), 1492-1500. doi:10.1093/ecco-jcc/jjz094

Gyorgy, B., Szabo, T. G., Pasztoi, M., Pal, Z., Misjak, P., Aradi, B., . . . Buzas, E. I. (2011). Membrane vesicles, current state-of-the-art: emerging role of extracellular vesicles. *Cell Mol Life Sci, 68*(16), 2667-2688. doi:10.1007/s00018-011-0689-3

Haga, H., Yan, I. K., Takahashi, K., Wood, J., Zubair, A., & Patel, T. (2015). Tumour cell-derived extracellular vesicles interact with mesenchymal stem cells to modulate the microenvironment and enhance cholangiocarcinoma growth. *J Extracell Vesicles, 4*, 24900. doi:10.3402/jev.v4.24900

Han, J. Y., Ahn, K. S., Baek, W. K., Suh, S. I., Kim, Y. H., Kim, T. S., & Kang, K. J. (2020). Usefulness of bile as a biomarker via ferroptosis and cysteine prenylation in cholangiocarcinoma; role of diagnosis and differentiation from benign biliary disease. *Surg Oncol, 34*, 174-181. doi:10.1016/j.suronc.2020.04.019

Harel, S., Sanchez-Gonzalez, V., Echavarria, R., Mayaki, D., & Hussain, S. N. (2020). Roles of miR-640 and Zinc Finger Protein 91 (ZFP91) in Angiopoietin-1-Induced In Vitro Angiogenesis. *Cells, 9*(7). doi:10.3390/cells9071602

Hoshino, A., Kim, H. S., Bojmar, L., Gyan, K. E., Cioffi, M., Hernandez, J., . . . Lyden, D. (2020). Extracellular Vesicle and Particle Biomarkers Define Multiple Human Cancers. *Cell, 182*(4), 1044-1061 e1018. doi:10.1016/j.cell.2020.07.009

Iorio, M. V., & Croce, C. M. (2012). Causes and consequences of microRNA dysregulation. *Cancer J, 18*(3), 215-222. doi:10.1097/PPO.0b013e318250c001

Izon. (2019). qEV2 User Manual. Retrieved from https://support.izon.com/technical-note-qev2 [last accessed: 15.03.2022]

Jiang, J., Ma, B., Li, X., Jin, W., Han, C., Wang, L., & Wang, H. (2018). MiR-1281, a p53-responsive microRNA, impairs the survival of human osteosarcoma cells upon ER stress via targeting USP39. *Am J Cancer Res, 8*(9), 1764-1774.

Julich-Haertel, H., Urban, S. K., Krawczyk, M., Willms, A., Jankowski, K., Patkowski, W., . . . Kornek, M. (2017). Cancer-associated circulating large extracellular vesicles in cholangiocarcinoma and hepatocellular carcinoma. *J Hepatol, 67*(2), 282-292. doi:10.1016/j.jhep.2017.02.024

Kai, Y., Ikezawa, K., Takada, R., Daiku, K., Maeda, S., Abe, Y., . . . Ohkawa, K. (2021). Success rate of microsatellite instability examination and complete response with pembrolizumab in biliary tract cancer. *JGH Open, 5*(6), 712-716. doi:10.1002/jgh3.12576

Kang, S., El-Rayes, B. F., & Akce, M. (2022). Evolving Role of Immunotherapy in Advanced Biliary Tract Cancers. *Cancers (Basel), 14*(7). doi:10.3390/cancers14071748

Kendall, T., Verheij, J., Gaudio, E., Evert, M., Guido, M., Goeppert, B., & Carpino, G. (2019). Anatomical, histomorphological and molecular classification of cholangiocarcinoma. *Liver Int, 39 Suppl 1*, 7-18. doi:10.1111/liv.14093

Khan, S. A., Tavolari, S., & Brandi, G. (2019). Cholangiocarcinoma: Epidemiology and risk factors. *Liver Int, 39 Suppl 1*, 19-31. doi:10.1111/liv.14095

Kim, A., Ng, W. B., Bernt, W., & Cho, N. J. (2019). Validation of Size Estimation of Nanoparticle Tracking Analysis on Polydisperse Macromolecule Assembly. *Sci Rep, 9*(1), 2639. doi:10.1038/s41598-019-38915-x

Lapitz, A., Arbelaiz, A., Olaizola, P., Aranburu, A., Bujanda, L., Perugorria, M. J., & Banales, J. M. (2018). Extracellular Vesicles in Hepatobiliary Malignancies. *Front Immunol, 9*, 2270. doi:10.3389/fimmu.2018.02270

Lapitz, A., Azkargorta, M., Milkiewicz, P., Olaizola, P., Zhuravleva, E., Grimsrud, M. M., . . . Banales, J. M. (2023). Liquid biopsy-based protein biomarkers for risk prediction, early diagnosis, and prognostication of cholangiocarcinoma. *J Hepatol, 79*(1), 93-108. doi:10.1016/j.jhep.2023.02.027

Letelier, P., Riquelme, I., Hernandez, A. H., Guzman, N., Farias, J. G., & Roa, J. C. (2016). Circulating MicroRNAs as Biomarkers in Biliary Tract Cancers. *Int J Mol Sci, 17*(5). doi:10.3390/ijms17050791

Lewis, J. T., Talwalkar, J. A., Rosen, C. B., Smyrk, T. C., & Abraham, S. C. (2010). Precancerous bile duct pathology in end-stage primary sclerosing cholangitis, with and without cholangiocarcinoma. *Am J Surg Pathol, 34*(1), 27-34. doi:10.1097/PAS.0b013e3181bc96f9

Li, L., Masica, D., Ishida, M., Tomuleasa, C., Umegaki, S., Kalloo, A. N., . . . Selaru, F. M. (2014). Human bile contains microRNA-laden extracellular vesicles that can be used for cholangiocarcinoma diagnosis. *Hepatology, 60*(3), 896-907. doi:10.1002/hep.27050

Li, L., Piontek, K. B., Kumbhari, V., Ishida, M., & Selaru, F. M. (2016). Isolation and Profiling of MicroRNA-containing Exosomes from Human Bile. *J Vis Exp*(112). doi:10.3791/54036

Li, X., Lu, Y., Chen, Y., Lu, W., & Xie, X. (2013). MicroRNA profile of paclitaxel-resistant serous ovarian carcinoma based on formalin-fixed paraffin-embedded samples. *BMC Cancer, 13*(1), 216. doi:10.1186/1471-2407-13-216

Lindkvist, B., Benito de Valle, M., Gullberg, B., & Bjornsson, E. (2010). Incidence and prevalence of primary sclerosing cholangitis in a defined adult population in Sweden. *Hepatology, 52*(2), 571-577. doi:10.1002/hep.23678

Liu, D. S. K., Upton, F. M., Rees, E., Limb, C., Jiao, L. R., Krell, J., & Frampton, A. E. (2020). Size-Exclusion Chromatography as a Technique for the Investigation of Novel Extracellular Vesicles in Cancer. *Cancers (Basel), 12*(11). doi:10.3390/cancers12113156

Liu, G., Jiang, Z., Qiao, M., & Wang, F. (2019). Lnc-GIHCG promotes cell proliferation and migration in gastric cancer through miR- 1281 adsorption. *Mol Genet Genomic Med, 7*(6), e711. doi:10.1002/mgg3.711

Liwinski, T., & Schramm, C. (2018). [Primary sclerosing cholangitis : Current diagnostics and treatment]. *Internist (Berl), 59*(6), 551-559. doi:10.1007/s00108-018-0428-z

Lu, J., Getz, G., Miska, E. A., Alvarez-Saavedra, E., Lamb, J., Peck, D., . . . Golub, T. R. (2005). MicroRNA expression profiles classify human cancers. *Nature, 435*(7043), 834-838. doi:10.1038/nature03702

Lv, H., Zhou, D., & Liu, G. (2021). LncRNA LINC00963 promotes colorectal cancer cell proliferation and metastasis by regulating miR-1281 and TRIM65. *Mol Med Rep, 24*(5). doi:10.3892/mmr.2021.12421

Maroto, R., Zhao, Y., Jamaluddin, M., Popov, V. L., Wang, H., Kalubowilage, M., . . . Brasier, A. R. (2017). Effects of storage temperature on airway exosome integrity for diagnostic and functional analyses. *J Extracell Vesicles, 6*(1), 1359478. doi:10.1080/20013078.2017.1359478

Moazzami, B., Majidzadeh, A. K., Dooghaie-Moghadam, A., Eslami, P., Razavi-Khorasani, N., Iravani, S., . . . Nassiri Toosi, M. (2020). Cholangiocarcinoma: State of the Art. *J Gastrointest Cancer, 51*(3), 774-781. doi:10.1007/s12029-020-00390-3

Nakanuma, Y., Sato, Y., Harada, K., Sasaki, M., Xu, J., & Ikeda, H. (2010). Pathological classification of intrahepatic cholangiocarcinoma based on a new concept. *World J Hepatol, 2*(12), 419-427. doi:10.4254/wjh.v2.i12.419

Nakashiki, S., Miuma, S., Mishima, H., Masumoto, H., Hidaka, M., Soyama, A., . . . Nakao, K. (2021). Bile extracellular vesicles from end-stage liver disease patients show altered microRNA content. *Hepatol Int, 15*(3), 821-830. doi:10.1007/s12072-021-10196-5

Navajas, R., Corrales, F. J., & Paradela, A. (2019). Serum Exosome Isolation by Size-Exclusion Chromatography for the Discovery and Validation of Preeclampsia-Associated Biomarkers. *Methods Mol Biol, 1959*, 39-50. doi:10.1007/978-1-4939-9164-8_3

Nordin, J. Z., Lee, Y., Vader, P., Mager, I., Johansson, H. J., Heusermann, W., . . . El Andaloussi, S. (2015). Ultrafiltration with size-exclusion liquid chromatography for high yield isolation of extracellular vesicles preserving intact biophysical and functional properties. *Nanomedicine, 11*(4), 879-883. doi:10.1016/j.nano.2015.01.003

Novikov, A., Kowalski, T. E., & Loren, D. E. (2019). Practical Management of Indeterminate Biliary Strictures. *Gastrointest Endosc Clin N Am, 29*(2), 205-214. doi:10.1016/j.giec.2018.12.003

Olaizola, P., Lee-Law, P. Y., Arbelaiz, A., Lapitz, A., Perugorria, M. J., Bujanda, L., & Banales, J. M. (2018). MicroRNAs and extracellular vesicles in cholangiopathies. *Biochim Biophys Acta Mol Basis Dis, 1864*(4 Pt B), 1293-1307. doi:10.1016/j.bbadis.2017.06.026

Park, S., Lee, K., Park, I. B., Kim, N. H., Cho, S., Rhee, W. J., . . . Lee, D. H. (2020). The profiles of microRNAs from urinary extracellular vesicles (EVs) prepared by various isolation methods and their correlation with serum EV microRNAs. *Diabetes Res Clin Pract, 160*, 108010. doi:10.1016/j.diabres.2020.108010

Pignot, G., Cizeron-Clairac, G., Vacher, S., Susini, A., Tozlu, S., Vieillefond, A., . . . Bieche, I. (2013). microRNA expression profile in a large series of bladder tumors: identification of a 3-miRNA signature associated with aggressiveness of muscle-invasive bladder cancer. *Int J Cancer, 132*(11), 2479-2491. doi:10.1002/ijc.27949

Ramirez, M. I., Amorim, M. G., Gadelha, C., Milic, I., Welsh, J. A., Freitas, V. M., . . . Dias-Neto, E. (2018). Technical challenges of working with extracellular vesicles. *Nanoscale, 10*(3), 881-906. doi:10.1039/c7nr08360b

Rodriguez-Caro, H., Dragovic, R., Shen, M. N., Dombi, E., Mounce, G., Field, K., . . . Granne, I. (2019). decidualisation of human endometrial stromal cells is enhanced by seminal fluid extracellular vesicles. *Journal of extracellular vesicles, 8*(1), 1565262. doi:A10.1080/20013078.2019.1565262

Roest, H. P., Verhoeven, C. J., & van der Laan, L. J. (2015). MicroRNAs in bile vesicles: finding a trade-off for biomarker discovery. *Hepatology, 61*(3), 1094-1095. doi:10.1002/hep.27325

Royo, F., Thery, C., Falcon-Perez, J. M., Nieuwland, R., & Witwer, K. W. (2020). Methods for Separation and Characterization of Extracellular Vesicles: Results of a Worldwide Survey Performed by the ISEV Rigor and Standardization Subcommittee. *Cells, 9*(9). doi:10.3390/cells9091955

Saffioti, F., Roccarina, D., Vesterhus, M., Hov, J. R., Rosenberg, W., Pinzani, M., . . . Thorburn, D. (2019). Cholangiocarcinoma is associated with a raised enhanced liver fibrosis score independent of primary sclerosing cholangitis. *Eur J Clin Invest, 49*(5), e13088. doi:10.1111/eci.13088

Sarker, S., Scholz-Romero, K., Perez, A., Illanes, S. E., Mitchell, M. D., Rice, G. E., & Salomon, C. (2014). Placenta-derived exosomes continuously increase in maternal circulation over the first trimester of pregnancy. *J Transl Med, 12*, 204. doi:10.1186/1479-5876-12-204

Severino, V., Dumonceau, J. M., Delhaye, M., Moll, S., Annessi-Ramseyer, I., Robin, X., . . . Farina, A. (2017). Extracellular Vesicles in Bile as Markers of Malignant Biliary Stenoses. *Gastroenterology, 153*(2), 495-504 e498. doi:10.1053/j.gastro.2017.04.043

Shah, S. C., Ten Hove, J. R., Castaneda, D., Palmela, C., Mooiweer, E., Colombel, J. F., . . . Torres, J. (2018). High Risk of Advanced Colorectal Neoplasia in Patients With Primary Sclerosing Cholangitis Associated With Inflammatory Bowel Disease. *Clin Gastroenterol Hepatol, 16*(7), 1106-1113.e1103. doi:10.1016/j.cgh.2018.01.023

Shao, H., Im, H., Castro, C. M., Breakefield, X., Weissleder, R., & Lee, H. (2018). New Technologies for Analysis of Extracellular Vesicles. *Chem Rev, 118*(4), 1917-1950. doi:10.1021/acs.chemrev.7b00534

Shigehara, K., Yokomuro, S., Ishibashi, O., Mizuguchi, Y., Arima, Y., Kawahigashi, Y., . . . Uchida, E. (2011). Real-time PCR-based analysis of the human bile microRNAome identifies miR-9 as a potential diagnostic biomarker for biliary tract cancer. *PLoS One, 6*(8), e23584. doi:10.1371/journal.pone.0023584

Singh, A., Gelrud, A., & Agarwal, B. (2015). Biliary strictures: diagnostic considerations and approach. *Gastroenterol Rep (Oxf), 3*(1), 22-31. doi:10.1093/gastro/gou072

Son, K. H., Ahn, C. B., Kim, H. J., & Kim, J. S. (2020). Quantitative proteomic analysis of bile in extrahepatic cholangiocarcinoma patients. *J Cancer, 11*(14), 4073-4080. doi:10.7150/jca.40964

Song, J., Li, Y., Bowlus, C. L., Yang, G., Leung, P. S. C., & Gershwin, M. E. (2020). Cholangiocarcinoma in Patients with Primary Sclerosing Cholangitis (PSC): a Comprehensive Review. *Clin Rev Allergy Immunol, 58*(1), 134-149. doi:10.1007/s12016-019-08764-7

Stevic, I., Buescher, G., & Ricklefs, F. L. (2020). Monitoring Therapy Efficiency in Cancer through Extracellular Vesicles. *Cells, 9*(1). doi:10.3390/cells9010130

Stranska, R., Gysbrechts, L., Wouters, J., Vermeersch, P., Bloch, K., Dierickx, D., . . . Snoeck, R. (2018). Comparison of membrane affinity-based method with size-exclusion chromatography for isolation of exosome-like vesicles from human plasma. *J Transl Med, 16*(1), 1. doi:10.1186/s12967-017-1374-6

Taghavi, S. A., Eshraghian, A., Niknam, R., Sivandzadeh, G. R., & Bagheri Lankarani, K. (2018). Diagnosis of cholangiocarcinoma in primary sclerosing cholangitis. *Expert Rev Gastroenterol Hepatol, 12*(6), 575-584. doi:10.1080/17474124.2018.1473761

Tang, C., Wang, X., Ji, C., Zheng, W., Yu, Y., Deng, X., . . . Fang, L. (2021). The Role of miR-640: A Potential Suppressor in Breast Cancer via Wnt7b/β-catenin Signaling Pathway. *Front Oncol, 11*, 645682. doi:10.3389/fonc.2021.645682

Turchinovich, A., Weiz, L., & Burwinkel, B. (2012). Extracellular miRNAs: the mystery of their origin and function. *Trends Biochem Sci, 37*(11), 460-465. doi:10.1016/j.tibs.2012.08.003

Valle, J. W., Wasan, H., Johnson, P., Jones, E., Dixon, L., Swindell, R., . . . Bridgewater, J. (2009). Gemcitabine alone or in combination with cisplatin in patients with advanced or metastatic cholangiocarcinomas or other biliary tract tumours: a multicentre randomised phase II study - The UK ABC-01 Study. *Br J Cancer, 101*(4), 621-627. doi:10.1038/sj.bjc.6605211

Vaswani, K., Mitchell, M. D., Holland, O. J., Qin Koh, Y., Hill, R. J., Harb, T., . . . Peiris, H. (2019). A Method for the Isolation of Exosomes from Human and Bovine Milk. *J Nutr Metab, 2019*, 5764740. doi:10.1155/2019/5764740

Vergauwen, G., Dhondt, B., Van Deun, J., De Smedt, E., Berx, G., Timmerman, E., . . . Hendrix, A. (2017). Confounding factors of ultrafiltration and protein analysis in extracellular vesicle research. *Sci Rep, 7*(1), 2704. doi:10.1038/s41598-017-02599-y

Vogel, A., Bridgewater, J., Edeline, J., Kelley, R. K., Klumpen, H. J., Malka, D., . . . clinicalguidelines@esmo.org, E. G. C. E. a. (2023). Biliary tract cancer: ESMO Clinical Practice Guideline for diagnosis, treatment and follow-up. *Ann Oncol, 34*(2), 127-140. doi:10.1016/j.annonc.2022.10.506

Voigtlander, T., Gupta, S. K., Thum, S., Fendrich, J., Manns, M. P., Lankisch, T. O., & Thum, T. (2015). MicroRNAs in Serum and Bile of Patients with Primary Sclerosing Cholangitis and/or Cholangiocarcinoma. *PLoS One, 10*(10), e0139305. doi:10.1371/journal.pone.0139305

Voigtlander, T., & Lankisch, T. O. (2015). Endoscopic diagnosis of cholangiocarcinoma: From endoscopic retrograde cholangiography to bile proteomics. *Best Pract Res Clin Gastroenterol, 29*(2), 267-275. doi:10.1016/j.bpg.2015.02.005

Voigtlander, T., Metzger, J., Schonemeier, B., Jager, M., Mischak, H., Manns, M. P., & Lankisch, T. O. (2017). A combined bile and urine proteomic test for cholangiocarcinoma diagnosis in patients with biliary strictures of unknown

origin. *United European Gastroenterol J, 5*(5), 668-676. doi:10.1177/2050640616687836

Wang, Y., Wei, H., Song, L., Xu, L., Bao, J., & Liu, J. (2020). Gene Expression Microarray Data Meta-Analysis Identifies Candidate Genes and Molecular Mechanism Associated with Clear Cell Renal Cell Carcinoma. *Cell J, 22*(3), 386-393. doi:10.22074/cellj.2020.6561

Weismüller, T. J., Trivedi, P. J., Bergquist, A., Imam, M., Lenzen, H., Ponsioen, C. Y., . . . Boberg, K. M. (2017). Patient Age, Sex, and Inflammatory Bowel Disease Phenotype Associate With Course of Primary Sclerosing Cholangitis. *Gastroenterology, 152*(8), 1975-1984.e1978. doi:10.1053/j.gastro.2017.02.038

Witwer, K. W., Buzas, E. I., Bemis, L. T., Bora, A., Lasser, C., Lotvall, J., . . . Hochberg, F. (2013). Standardization of sample collection, isolation and analysis methods in extracellular vesicle research. *J Extracell Vesicles, 2*. doi:10.3402/jev.v2i0.20360

Xie, C., Aloreidi, K., Patel, B., Ridgway, T., Thambi-Pillai, T., Timmerman, G., . . . Atiq, M. (2018). Indeterminate biliary strictures: a simplified approach. *Expert Rev Gastroenterol Hepatol, 12*(2), 189-199. doi:10.1080/17474124.2018.1391090

Yan, I. K., Berdah, V. X., & Patel, T. (2018). Isolation of Extracellular RNA from Bile. *Methods Mol Biol, 1740*, 59-67. doi:10.1007/978-1-4939-7652-2_6

Yan, S., Han, B., Gao, S., Wang, X., Wang, Z., Wang, F., . . . Sun, B. (2017). Exosome-encapsulated microRNAs as circulating biomarkers for colorectal cancer. *Oncotarget, 8*(36), 60149-60158. doi:10.18632/oncotarget.18557

Yoon, S. B., & Chang, J. H. (2017). Extracellular vesicles in bile: a game changer in the diagnosis of indeterminate biliary stenoses? *Hepatobiliary Surg Nutr, 6*(6), 408-410. doi:10.21037/hbsn.2017.10.01

Zhai, Z., Fu, Q., Liu, C., Zhang, X., Jia, P., Xia, P., . . . Zhang, H. (2019). Emerging Roles Of hsa-circ-0046600 Targeting The miR-640/HIF-1α Signalling Pathway In The Progression Of HCC. *Onco Targets Ther, 12*, 9291-9302. doi:10.2147/ott.S229514

Zhang, H., Zhu, M., Shan, X., Zhou, X., Wang, T., Zhang, J., . . . Zhu, W. (2019). A panel of seven-miRNA signature in plasma as potential biomarker for colorectal cancer diagnosis. *Gene, 687*, 246-254. doi:10.1016/j.gene.2018.11.055

Figure table

Figure number	Original title	Reference + page
Figure 1	Figure 1	(Kendall et al., 2019), page 9
Figure 2	Fig. 3	(Gyorgy et al., 2011), page 2670
Figure 3	Figure 3B	(Choi et al., 2015), page 3
Figure 4	Figure 1	(D. S. K. Liu et al., 2020), page 3
Figure 5	Figure 1	(Turchinovich et al., 2012), page 461
Figure 7	Figure 2	(D. S. K. Liu et al., 2020), page 13
Figure 8	Figure 6 (a)	(Kim et al., 2019), page 8

11. List of Abbreviations

AGO	argonaut protein
AIH	autoimmune hepatitis
ALT	alanine aminotransferase
ANA	anti-mitochondrial antibody
AP	alkaline phosphatase
AST	aspartate aminotransferase
AUC	area under the ROC curve
BCA	bicinchoninic acid
BiIIN	Biliary intraepithelial neoplasia
BMI	body mass index
BSA	bovine serum albumin
CA19-9	carbohydrate antigen 19-9
CCA	cholangiocarcinoma
CRP	c-reactive protein
CT	computed tomography
dCCA	distal cholangiocarcinoma
DLS	dynamic light scattering
EASL	European Association for the Study of the Liver
eCCA	extrahepatic cholangiocarcinoma
ELISZA	enzyme-linked immunosorbent assay
ERCP	endoscopic retrograde cholangiopancreatography
ESGE	European Society of Gastroenterology
EUS	endoscopic ultrasound
EV	extracellular vesicle
FISH	fluorescence in situ hybridisation
FNA	fine needle aspiration
HDL	high density lipoproteins
HIF	hypoxia-induced factor
iCCA	intrahepatic cholangiocarcinoma
IDB	inflammatory bowel disease
LC-MS	liquid chromatography–mass spectrometry

MRCP	magnetic resonance cholangiopancreatography
MRI	magnetic resonance imaging
NTA	nanoparticle tracking analysis
OLT	orthotopic liver transplantation
p-ANCA	perinuclear anti-neutrophil cytoplasmic antibodies
PBS	phosphate buffered saline
PCA	pancreatic carcinoma
pCCA	peripheral cholangiocarcinoma
PSC	primary sclerosing cholangitis
PSC-CCA	PSC-associated cholangiocarcinoma
PTCD	percutaneous transhepatic cholangiodrainage
qPCR	quantitative polymerase chain reaction
RISC	RNA-induced silencing complex
RT-PCR	real time polymerase chain reaction
SEC	size exclusion chromatography
SMA	smooth muscle antibody
SNARE	soluble N-ethylmaleimide-sensitive-factor attachment receptor
TACE	transarterial chemoembolization
TEM	transmissions electron microscopy
TSG 101	tumor susceptibility gene 101 protein
UC	ultracentrifugation
UDCA	ursodeoxycholic acid
UF	ultrafiltration
UICC	Union for International Cancer Control
WB	western blot
yGT	gamma-guanyltransferase

12. Funding

This study was kindly supported by the KFO306.

13. Danksagung

Vielen Dank an all die Menschen, die mich während dieser Zeit und darüber hinaus unterstützt haben!

Meinem Doktorvater Prof. Dr. Christoph Schramm möchte ich einen großen Dank aussprechen für jegliche Unterstützung und Begleitung meiner Arbeit und das stets konstruktive und wertvolle Feedback. Ein ganz besonderer Dank geht an Dr. Jenny Krause für die tolle Betreuung, die lösungsorientierten und positiven Meetings und die unermüdliche Unterstützung. Es hat wirklich Spaß gemacht mit Dir zu arbeiten. Auch Dr. Gustav Büscher danke ich für die wertvollen Tipps und Ratschläge.

Der KFO306 möchte ich für die Finanzierung des Forschungsprojektes danken. Außerdem dem ganzen Team des Graduiertenkollegs „Entzündung und Regeneration“ des SFB841 vom UKE unter der Leitung von Prof. Dr. Gisa Tiegs für die finanzielle Unterstützung, die tollen Workshops sowie die für die Organisation der zahlreichen Ringvorlesungen und Journal Clubs.

Vielen Dank an die ganze AG Herkel/Schramm, insbesondere Sabrina Kreß, Jennifer Wigger, Gela Schmidt, Marko Hilken und Nina Verse, für ihre immer freundliche, immer optimistische und immer geduldige Hilfsbereitschaft. Außerdem ein Dank an Martina Fahl aus der AG Schrader für die liebe Unterstützung beim Western Blotting.

Für die Bereitstellung der Galleproben danke ich der Abteilung für Interventionelle Endoskopie am UKE und für die Einführung in die NTA danke ich Dr. Mohsin Shafiq aus dem Institut für Neuropathologie. Carola Schneider aus dem Heinrich-Pette-Institut danke ich für die TEM-Bilder und Ihre Anleitung zum Negative Staining. Auch Hannah Voß aus der AG Schlüter möchte ich für ihre Bemühungen um eine Proteomanalyse danken.

Letztlich ein riesiger Dank an meine Familie und Freunde. Ich verdanke euch so viel!

14. Lebenslauf

Der Lebenslauf wurde aus datenschutztechnischen Gründen entfernt.

15. Eidesstattliche Erklärung

Ich versichere ausdrücklich, dass ich die Arbeit selbständig und ohne fremde Hilfe verfasst, andere als die von mir angegebenen Quellen und Hilfsmittel nicht benutzt und die aus den benutzten Werken wörtlich oder inhaltlich entnommenen Stellen einzeln nach Ausgabe (Auflage und Jahr des Erscheinens), Band und Seite des benutzten Werkes kenntlich gemacht habe. Ferner versichere ich, dass ich die Dissertation bisher nicht einem Fachvertreter an einer anderen Hochschule zur Überprüfung vorgelegt oder mich anderweitig um Zulassung zur Promotion beworben habe. Ich erkläre mich einverstanden, dass meine Dissertation vom Dekanat der Medizinischen Fakultät mit einer gängigen Software zur Erkennung von Plagiaten überprüft werden kann.

Unterschrift: .....